



1 **Diversity of intact polar lipids in the oxygen minimum zone of the Eastern Tropical North Pacific:**

2 **Biogeochemical implications of non-phosphorus lipids**

3 Florence Schubotz <sup>1\*</sup>, Sitan Xie <sup>1,¶</sup>, Julius S. Lipp <sup>1</sup>, Kai-Uwe Hinrichs <sup>1</sup>, Stuart G. Wakeham <sup>2</sup>

4

5

6 <sup>1</sup>MARUM and Department of Geosciences, University of Bremen, 28359 Bremen, Germany

7 <sup>2</sup>Skidaway Institute of Oceanography, Savannah, GA 31411, USA

8 <sup>¶</sup>Current address: Wai Gao Qiao Free Trade Zone, 200131 Shanghai, China

9

10

11

12

13

14

15

16

17 \*Corresponding author. MARUM, University of Bremen, Leobener Str. 13, Room 1070, 28359 Bremen,

18 Germany. Tel: +49-421-218-65724. Fax: +49-421-218-65715. E-mail: [schubotz@uni-bremen.de](mailto:schubotz@uni-bremen.de)

19

20 **Keywords:** intact polar lipids, phospholipids, glycolipids, betaine lipids, ether lipids, oxylipins,

21 phospholipid substitution, oxygen minimum zone



## 22 **Abstract**

23 Intact polar lipids (IPLs) are the main building blocks of cellular membranes and contain  
24 chemotaxonomic, ecophysiological and metabolic information, which makes them valuable biomarkers in  
25 microbial ecology and biogeochemistry. This study investigates the IPL distribution in suspended  
26 particulate matter (SPM) in the water column of the Eastern Tropical North Pacific Ocean (ETNP), an  
27 area characterized by one of the most extensive open ocean oxygen minimum zones (OMZ) in the world  
28 with strong gradients of nutrients, temperature and redox conditions. A wide structural variety in polar  
29 lipid head group composition and core structures exists along physical and geochemical gradients within  
30 the OMZ. Our goal is to use this structural diversity in IPLs to evaluate the microbial ecology and  
31 ecophysiological adaptations that affect organisms inhabiting the OMZ in the context of biogeochemical  
32 cycles. Diacylglycerol phospholipids are present at all depths, but exhibit highest relative abundance  
33 and compositional variety (including mixed acyl/ether core structures) in the upper and core OMZ where  
34 prokaryotic biomass was enriched. Surface ocean SPM is dominated by diacylglycerol glycolipids that  
35 are typical lipid components of photosynthetic membranes. These and other glycolipids with varying  
36 core structures composed of ceramides and hydroxylated fatty acids are also detected with varying relative  
37 abundances in the OMZ and deep oxycline, signifying additional non-phototrophic bacterial sources for  
38 these lipids. Similarly, betaine lipids (with none or multiple hydroxylations in the core structures) that  
39 are typically assigned to microalgae are found throughout the water column down to the deep oxycline  
40 but do not show a depth-related trend in relative abundance. Archaeal IPLs comprised of glycosidic and  
41 mixed glycosidic-phosphatidic glycerol dibiphytanyl glycerol tetraethers (GDGTs) are most abundant in  
42 the upper OMZ where nitrate maxima point to ammonium oxidation, but increase in relative abundance



43 in the core OMZ and deep oxycline. The presence of abundant non-phosphorus lipids within the OMZ  
44 suggests that the indigenous microbes might be phosphorus limited at phosphate concentrations of 1 to  
45 3.5  $\mu\text{M}$ . It remains unclear if the detected amino and glycolipids indeed function as substitutes for  
46 phospholipid in these oxygen-depleted environments as microbial sources for many of these lipids still  
47 remain unknown.



## 48 **1. Introduction**

49       Oxygen Minimum Zones (OMZ, first coined by Richards, 1965) are permanently oxygen-deficient  
50 regions in the ocean defined by O<sub>2</sub> concentrations <20 μM. They primarily occur in areas where coastal  
51 or open ocean upwelling of cold, nutrient-rich waters drive elevated levels of primary production and  
52 subsequent respiration of organic matter exported out of productive surface waters consumes oxygen  
53 faster than it is replaced by ventilation or by mid-depth lateral injections of oxygenated water. OMZs  
54 are generally considered as “dead zones” in which low oxygen levels cause habitat compression, whereby  
55 species intolerant to low levels of oxygen are restricted to oxygenated surface waters (Keeling et al., 2010;  
56 Rush et al., 2012). But even these low levels of oxygen permit vertical migration of some zooplankton  
57 taxa into hypoxic waters (e.g., Wishner et al., 2013), although metabolic rates are greatly suppressed (e.g.,  
58 Seibel, 2011). Oxygen depletion also stimulates diverse microbial life capable of utilizing alternative  
59 electron acceptors for respiration under microaerobic conditions (e.g., Ulloa et al., 2012; Tiano et al., 2014;  
60 Carolan et al., 2015; Kalvelage et al., 2015; Duret et al., 2015). Important prokaryote-mediated  
61 remineralization processes within OMZs include denitrification and the anaerobic oxidation of ammonium  
62 (anammox), which together may account for 30-50% of the total nitrogen loss from the ocean to the  
63 atmosphere (Gruber, 2008; Lam and Kuypers, 2011). Modern day OMZs comprise ~8% of global ocean  
64 volume (Karstensen et al., 2008; Paulmier and Ruiz-Pino, 2009; Lam and Kuypers, 2011), but any  
65 expansion in the coming decades as a consequence of global warming and increased stratification  
66 (Stramma et al., 2008; Keeling et al., 2010) would have profound effects on marine ecology, oceanic  
67 productivity, global carbon and nitrogen cycles, the biological pump and sequestration of carbon  
68 (Karstensen et al., 2008; Stramma et al., 2010; Wright et al., 2012). A better understanding of the effect



69 of low-O<sub>2</sub> on marine biogeochemistry and microbial ecology is thus warranted.

70 The Eastern Tropical North Pacific Ocean (ETNP) off the west coast of Mexico and Central America  
71 hosts one of the largest OMZs in the open ocean, extending halfway across the Pacific Ocean and  
72 comprising ~41% of global OMZs (Lavín and Fiedler, 2006; Fiedler and Talley, 2006; Paulmier and Ruiz-  
73 Pino, 2009). By comparison, the OMZs of the Eastern Tropical South Pacific Ocean (ETSP) off Peru  
74 and Chile and in the Arabian Sea are ~14% and ~8%, respectively, of global OMZs. In the ETNP, a  
75 sharp permanent pycnocline develops where warm, saline surface waters lie on top of a shallow  
76 thermocline, producing a highly stratified water column. Moderate primary production, dominated by  
77 picoplankton, depends on oceanic upwelling and wind mixing of coastal waters but is generally limited  
78 by lack of micronutrient dissolved iron (Franck et al., 2005; Pennington et al., 2006). Remineralization,  
79 ~70% of which is microbially mediated (Cavan et al., 2017), of particulate organic carbon exported out of  
80 surface waters consumes oxygen at rates that cannot be balanced by ventilation across the pycnocline and  
81 by sluggish lateral circulation, leading to O<sub>2</sub> levels as low as 0.1 μM at depths between ~100 and ~800 m.  
82 Abundances of micro- (Olson and Daly, 2013) and macro-zooplankton (Wishner et al., 2013; Williams et  
83 al., 2014) that are high in surface waters are reduced in the OMZ, and those macrozooplankton that are  
84 diel vertical migrators survive in the OMZ with reduced metabolic rates (Maas et al., 2014; Cass and Daly,  
85 2015). Microbial abundances and activities for both heterotrophic and chemoautotrophic metabolisms  
86 are high in both surface waters and within the OMZ, but again with reduced metabolic rates in the OMZ  
87 (Podlaska et al., 2012). A strong nutricline suggests microbial nitrogen cycling involving co-occurring  
88 nitrification, denitrification and anammox (Rush et al., 2012; Podlaska et al., 2012), perhaps contributing  
89 up to 45% of the global pelagic denitrification (Codispoti and Richards, 1976). Microbial communities



90 are mainly comprised of proteobacteria, with increasing contributions of crenarchaea in deeper waters.  
91 Yet, on average ca. 50% of the prokaryotic communities within the OMZ of the ETNP remained  
92 uncharacterized (Podlaska et al., 2012).

93 Intact polar lipids (IPLs) that are the main building blocks of cellular membranes may be used to  
94 characterize abundance and physiology of aquatic microorganisms from all three domains of life  
95 (Schubotz et al., 2009; Van Mooy et al., 2009; Pitcher et al., 2011; Popendorf, et al., 2011a). IPL  
96 distributions have been documented in surface waters of the Eastern Subtropical South Pacific (Van Mooy  
97 and Fredricks, 2010), the Western North Atlantic Ocean (Van Mooy et al., 2006; Popendorf, Lomas, et al.,  
98 2011a), the Mediterranean Sea (Popendorf, et al., 2011b), North Sea (Brandsma et al., 2012), lakes (Bale  
99 et al., 2016) and throughout the water column of stratified water bodies (Ertefai et al., 2008; Schubotz et  
100 al., 2009; Wakeham et al., 2012). Surface waters are typically dominated by nine different IPL classes.  
101 Three diacylglycerol glycolipids, monoglycosyl (1G-), diglycosyl (2G-) and sulfoquinovosyl  
102 diacylglycerol (SQ-DAG), are established photosynthetic markers as they are the main IPLs in all  
103 thylakoid membranes, including those of cyanobacteria (Siegenthaler et al., 1998). Generally abundant  
104 are also three classes of betaine lipids, diacylglyceryl homoserine (DGTS), hydroxymethyl-trimethyl- $\beta$ -  
105 alanine (DGTA) and carboxy-*N*-hydroxymethyl-choline (DGCC), which are widely distributed in lower  
106 plants and green algae (Dembitsky, 1996) and are thus typically assigned to eukaryotic algae in the ocean  
107 (Popendorf, et al., 2011a). Three commonly detected phospholipids are diacylglycerol phosphatidyl  
108 choline (PC), phosphatidyl ethanolamine (PE), and phosphatidyl glycerol (PG), all of which have mixed  
109 eukaryotic or bacterial sources in the upper water column (Sohlenkamp et al., 2003; Popendorf, et al.,  
110 2011a). These microbial source assignments have been broadly confirmed by isotope labeling studies



111 (Popendorf, et al., 2011a). Deeper in the water column of stratified water bodies the IPL distribution  
112 becomes more diverse and other phospholipids such as phosphatidyl (*N*)-methylethanolamine (PME),  
113 phosphatidyl (*N,N*)-dimethylethanolamine (PDME) and diphosphatidyl glycerol (DPG) become more  
114 abundant; these IPLs occur in a number of bacteria that may be present at these depths (cf. Schubotz et  
115 al., 2009; Wakeham et al., 2012). Several lipids with currently unknown bacterial sources have also been  
116 detected, including glycosidic ceramides or dietherglycerol phospholipids (Schubotz et al., 2009;  
117 Wakeham et al., 2012). Archaeal IPLs commonly found in the oceanic water column are glycosidic  
118 glycerol dialkyl glycerol tetraethers (GDGT) or mixed phospho-glyco head groups (Pitcher et al., 2011;  
119 Zhu et al., 2016). Abundances of archaeal GDGTs vary considerably with depth, but are typically  
120 elevated in zones of water column oxygen depletion (e.g., Black Sea, Wakeham et al., 2007; Schubotz et  
121 al., 2009; Cariaco Basin, Wakeham et al., 2012; off Cape Blanc, NE Atlantic, Basse et al., 2014; ETNP,  
122 Xie et al., 2014; ETSP, Sollai et al., 2015), especially where ammonium oxidizing thaumarchaea are  
123 abundant (Pitcher et al., 2011) or at greater depths where Marine Group II euryarchaea have been detected  
124 (Lincoln et al., 2014).

125 In addition to their use to phylogenetically classify major microbial groups, IPLs can be applied as  
126 metabolic and physiologic markers. Many organisms remodel their IPL composition when faced with  
127 environmental stressors such as changes in pH, salinity, temperature or availability of nutrients (Zhang  
128 and Rock, 2008; Van Mooy et al., 2009; Turich and Freeman, 2011; Meador et al., 2014; Carini et al.,  
129 2015; Elling et al., 2015; Hurley et al., 2016). Notably here, replacing phospholipids with non-  
130 phosphorus containing substitute lipids is an important mechanism when facing nutrient limitation in  
131 oligotrophic surface waters where phosphate concentrations reach nanomolar levels. Cyanobacteria



132 replace PG-DAG with SQ-DAG (Benning et al., 1993; Van Mooy et al., 2006), microalgae and some  
133 bacteria replace PC-DAG with DGTS (Geiger et al., 1999; Van Mooy et al., 2009; Popenorf, et al., 2011b)  
134 due to their similar ionic charge at physiological pH. Recently, it was also shown that marine  
135 heterotrophic bacteria replace PE-DAG with either 1G-DAG or DGTS (Carini et al., 2015; Sebastian et  
136 al., 2016; Yao et al., 2015). Such a dynamic response of membrane lipid composition to nutrient  
137 limitation has also been demonstrated for mixed planktonic communities in the environment (Van Mooy  
138 and Fredricks, 2010; Popenorf et al., 2011b).

139 In this study we use a complementary approach to study the microbial populations inhabiting the  
140 OMZ of the ETNP via the analysis of eukaryotic, bacterial and archaeal IPLs in SPM. This study is an  
141 extension of Xi et al. (2014), which focused on the detailed distribution of core and intact polar archaeal  
142 and bacterial tetraether lipids at two of stations (station 1 and 8) described here. There are distinct  
143 biogeochemical zonations within the water column of the ETNP based on IPL distributions which must  
144 reflect the localized ecology. Abundant non-phosphorus (substitute) lipids within the core of the OMZ  
145 might result from phosphorus limitation of the source microorganisms. Overall our results should  
146 provide deeper insight into the biogeochemical cycles and functioning of OMZs throughout the World  
147 Ocean.

148

## 149 **2. Methods**

### 150 *2.1 Sample collection and CTD data*

151 Suspended particulate matter (SPM) samples were collected at four stations (distance to shore:  
152 400~600 km; Fig 1) along a northwest-southeast transect (Station 1: 13°N, 105°W; Station 2: 12° 14' N,





153 101° 13.74' W; Station 5: 10° 41.41' N, 96° 56.6' W; and Station 8: 9°N, 90°W) in the ETNP during the  
154 R/V *Seward Johnson* cruise in November 2007 (R/V *Seward Johnson* Cruise Scientists, 2007). Station  
155 1 in the Tehuantepec Bowl is an area of relatively low primary productivity (e.g., 0.05 mg Chl-*a*/m<sup>2</sup>;  
156 (Fiedler and Talley, 2006; Pennington et al., 2006) whereas Station 8 in the Costa Rica Dome is moderately  
157 productive (1 mg Chl-*a*/m<sup>2</sup>). All stations are characterized by a strong thermocline/pycnocline/oxycline  
158 (at 20-50 m depths depending on location) and a profound and thick OMZ (down to ~2 μM O<sub>2</sub> between  
159 ~300-800 m depth). Station 1 is a reoccupation of the Vertical Transport and Exchange (VERTEX) II  
160 and II site that was intensely studied in the early 1980's (Martin et al., 1987), including several reports on  
161 organic biogeochemistry there (Lee and Cronin, 1984; Wakeham and Canuel, 1988; Wakeham 1987, 1989).

162 Seawater was filtered *in-situ* using submersible pumps (McLane Research Laboratories WTS-142  
163 filtration systems) deployed on the conducting cable of the CTD/rosette (Seabird 3+ temperature sensor,  
164 Seabird 9+ digital quartz pressure sensor, Seabird 4C conductivity sensor, Seabird 43 oxygen sensor, C-  
165 Point chlorophyll fluorescence sensor, Wetlabs CST-721DR 25 cm path length transmissometer).  
166 Volumes ranged between 130 and 1800 L. Temperature, conductivity, fluorescence and dissolved  
167 oxygen were measured during pump deployments and again during recovery; pump depths (4 pumps per  
168 cast) were monitored from the CTD depth during pumping. Pumps were fitted with two-tier 142 mm  
169 diameter filter holders: a 53 μm mesh Nitex “prefiltration” screen to remove most eukaryotes and marine  
170 snow aggregates and a double-stacked tier of ashed glass fiber filters (142 mm Gelman type A/E, nominal  
171 pore size 0.7 μm). It is likely that smaller cells (diameter 0.2-0.7 μm) were not retained on the filter and  
172 thus the reported IPL concentrations represent minimum values. After filtration, samples were wrapped  
173 in pre-combusted foil and stored frozen at -20°C until extraction.



174

175 *2.2 Elemental, pigment and nutrient analysis*

176 Particulate organic carbon (POC) and total particulate nitrogen (TN) were measured on 14 mm-diameter  
177 subsamples of each GFF prior to lipid extraction; therefore, POC and TN concentrations reported here are  
178 only for <53  $\mu\text{m}$  material. The plugs were acidified in HCl vapor in a desiccator for 12 hours to remove  
179 inorganic carbon. Elemental analysis was performed with a ThermoFinnigan Flash EA Series 1112  
180 interfaced to a ThermoFinnigan Delta V isotope ratio mass spectrometer at the Skidaway Institute  
181 Scientific Stable Isotope Laboratory (SISSIL). Organic carbon and nitrogen contents were calibrated  
182 against internal laboratory chitin powder standards which in turn had previously been cross-calibrated  
183 against USGS 40 and 41 international standards.

184 Two sets of pigment analyses were conducted. Chlorophyll-*a* (Chl-*a*) and pheopigment  
185 concentrations were measured on-board the ship (Olson and Daly, 2013). Seawater samples (100 – 500  
186 ml) from CTD casts were filtered onto Whatman GF/F filters which were immediately extracted with 90%  
187 acetone. Fluorescence was measure with a Turner Designs 10AU fluorometer and Chl-*a* concentrations  
188 were determined after Parsons et al (1984). Post-cruise HPLC analysis of pigments in 100-500 ml  
189 seawater samples filtered onto Whatman GF/F filters were conducted at the College of Charleston Grice  
190 Marine Laboratory, Charleston, SC on a Hewlett Packard 1050 system (DiTullio and Geesey, 2002).

191 Seawater samples for nutrient analyses ( $\text{NO}_2^-$ ,  $\text{NO}_3^{-2}$ ,  $\text{NH}_4^+$ ) were collected directly from Niskin  
192 bottles into acid-washed, 30-mL high-density polyethylene (HDP) bottles. After three rinses, bottles  
193 were filled to the shoulder, sealed, and frozen ( $-20^\circ\text{C}$ ). All frozen samples were transported to the  
194 Oceanic Nutrient Laboratory at USF for analysis using a Technicon Autoanalyzer II.



195

196 *2.3 Lipid extraction and analysis of intact polar lipids*

197 Lipids associated with the <math><53\ \mu\text{m}</math> SPM on the GFFs were Soxhlet-extracted using  
198 dichloromethane:methanol (DCM:MeOH; 9:1 v/v) for 8 h (Wakeham et al., 2007). Extracted lipids were  
199 partitioned into DCM against 5% NaCl solution and dried over  $\text{Na}_2\text{SO}_4$ . Total lipid extracts (TLEs) were  
200 stored at  $-20^\circ\text{C}$ .

201 An aliquot of the TLE was dissolved in DCM/Methanol (5:1 v/v) for analysis on a ThermoFinnigan  
202 Surveyor high-performance liquid chromatography system coupled to a ThermoFinnigan LCQ DecaXP  
203 Plus ion-trap mass spectrometer via electrospray interface (HPLC-ESI-IT-MS<sup>n</sup>) using conditions  
204 described previously (Sturt et al., 2004). Ten  $\mu\text{L}$  of an aliquot spiked with  $\text{C}_{19}$ -PC as internal standard  
205 was injected onto a LiChrosphere Diol-100 column ( $150 \times 2.1\ \text{mm}$ ,  $5\ \mu\text{m}$ , Alltech, Germany) equipped  
206 with a guard column of the same packing material. These data were used to obtain IPL concentrations.  
207 Sum formulas and IPL structures were assigned based on exact masses in the MS1 and MS-MS  
208 experiments during analysis of an aliquot of the TLE on a Bruker maXis Plus ultra-high resolution  
209 quadrupole time-of-flight mass spectrometer (Q-TOF) with an ESI source coupled to a Dionex Ultimate  
210 3000RS UHPLC. Separation of IPLs was achieved using a Waters Acquity UPLC BEH Amide column  
211 as described in (Wörmer et al., 2013). Selected samples were measured in positive and negative  
212 ionization modes with automated data-dependent fragmentation of base peak ions. Acyl moieties of  
213 glycolipids and aminolipids were identified via HPLC-IT-ESI-MS<sup>2</sup> experiments in positive ionization  
214 mode, and of phospholipids in negative ionization mode. Details of mass spectral interpretation, and  
215 identification of fatty acids moieties are described in Sturt et al. (2004) and Schubotz et al. (2009). For



216 all analyses, response factors of individual IPLs relative to the injection standard C<sub>19</sub>-PC could be  
217 determined for all major and some minor IPLs using commercially available standards: 1G-DAG, 2G-  
218 DAG, SQ-DAG, 1G-CER, DGTS, PG-DAG, DPG, PE-DAG, PME-DAG, PDME-DAG, PC-DAG, PC-  
219 DEG (Avanti Polar Lipids, USA) and 1G-PG-GDGT (Matreya LLC, USA). Some ions assigned to either  
220 PE-AEG and PC-AEG could not be quantified individually due to co-elution of these compounds and  
221 were thus quantified as one group using the mean response factor of PE- and PC-DAG. For compound  
222 classes for which no standards were available, such as PI-DAG, OL and the unknown aminolipids AL-I  
223 and AL-II the relative response could not be corrected for and values may thus be off by a factor of 0.2 to  
224 1.4, which is the maximum range of response factors observed for the standards.

225

#### 226 2.4 Statistical analysis

227 Nonmetric multidimensional scaling (NMDS) analysis was used to illustrate the relationships  
228 among objects hidden in a complex data matrix (Rabinowitz, 1975) and was performed in the free software  
229 R (version 3.4.3, [www.r-project.org/](http://www.r-project.org/)) with *metaMDS* (vegan library, version 2.4-6) as described by  
230 Wakeham et al. (2012). The datasets of relative lipid distribution and variations in chain length and  
231 unsaturation were standardized by Hellinger transformation using the function *decostand*, while for all  
232 other variables (environmental parameters, microbial groups) absolute numbers were used. The  
233 compositional dissimilarity was calculated by Euclidean distance measure. The resulting plot shows the  
234 distribution of lipids and sampling depths. Microbial groups and geochemical parameters were overlaid  
235 by function *envfit*. Lower stress is related to high quality of solution, and normally stress  $\leq 0.1$  is a  
236 guideline for good quality results (Rabinowitz, 1975). Non-parametric Spearman Rank Order



237 Correlation analysis was performed on combined data of environmental variables and IPL ratios and IPL  
238 relative abundances of all four stations using SigmaPlot 11.0 (Systat Software Inc., San Jose, USA).

239

### 240 **3. Results**

#### 241 *3.1 Biogeochemical setting*

242 All along the transect, the thin mixed layer (upper ~20 m) was warm, ~25 – 28 °C, with oxygen  
243 concentrations approaching air saturation at ~200 μM (Fig. 1b,c). The thermocline was abrupt at ~20-  
244 50 m, where temperatures dropped to ~15 – 18 °C and oxygen decreased to ~20 μM. Temperatures  
245 stabilized by ~250 – 300 m depth at ~10 – 12 °C and oxygen levels were <2 μM; especially at Station 8  
246 there were spatially and temporally variable oxygen intrusions into the upper portion of the OMZ. By  
247 ~600 – 800 m depth, a deep oxycline was observed where oxygen concentrations began to rise again to  
248 ~40 μM at temperatures of ~4 °C by 1250 m. Thus at the time of our cruise and for the purpose of this  
249 discussion, the water column of the ETNP could be roughly compartmentalized into four horizons based  
250 on oxygen content: an oxic epipelagic zone down to the thermocline (0 – 50 m; 200 μM > O<sub>2</sub> > 20 μM);  
251 an upper OMZ (Station 1 and 8: 50 – 300 m, Station 5: 50 – 350 m, Station 2: 50 – 200 m; 20 μM > O<sub>2</sub> >  
252 2 μM); the core OMZ (Station 1 and 8: 300 – 800 m, Station 5: 350 – 600 m Station 2: 200 – 600 m; O<sub>2</sub>  
253 < 2 μM); and a deep oxycline (Station 1 and 8 ≥ 800 m, Station 2 and 5 ≥ 600 m; O<sub>2</sub> > 2 μM) of rising O<sub>2</sub>  
254 levels (Fig. 1a).

255 Chl-*α* was highest in surface waters with maximum values of 1.8 μg/L at 10 m at station 5, were  
256 between 0.2 and 0.7 μg/L at station 2, 5 and 8 and decreased to values close to zero below 100 m at all  
257 stations (Fig. 1d; see also Fiedler and Talley, 2006, and Pennington et al., 2006, for additional results from



258 previous surveys). HPLC analysis of accessory pigments showed that picoplankton, primarily  
259 *Prochlorococcus* (indicated by divinyl chlorophyll  $\alpha$ ), were an important component of the  
260 photoautotrophic community, along with diatoms (fucoxanthin), especially *Rhizosolenia* at the deep  
261 fluorescence maximum at stations 1 and 5 but *Chaetoceros* at station 8, and prymnesiophytes  
262 (19'hexanoyloxyfucoxanthin and 19'butanoyloxyfucoxanthin; Suppl. Table 1). High phaeopigment  
263 abundances (up to 90% of [Chl- $\alpha$  + phaeopigments]) attested to algal senescence or grazing by macro-  
264 (Wishner et al., 2013; Williams et al. 2014) and micro-zooplankton (Olson and Daly, 2013) above and into  
265 the oxycline. Whereas the primary maxima in transmissivity (Beam C) corresponded with the peak Chl-  
266  $\alpha$  concentrations and fluorescence maxima, secondary transmissivity maxima were observed between 300  
267 and 400 m at stations 1, 5, and 8 indicating elevated particle abundances in the core of the OMZ (Fig. 1e).

268 Significant nitrite ( $\text{NO}_2^-$ ) maxima were observed in the OMZ at all stations coinciding with nitrate  
269 ( $\text{NO}_3^{2-}$ ) deficits (Fig. 2a,b). Ammonium ( $\text{NH}_4^+$ ) concentrations remained rather constant through the  
270 water column (Fig. 2c). Phosphate ( $\text{PO}_4^{3-}$ ; Fig. 2d) and total dissolved nitrogen (TDN; not shown) were  
271 low (respectively,  $< 0.5$  and  $< 3 \mu\text{M}$ ) in the upper 20 m of the oxic zone, but concentrations increase in  
272 the OMZ; both were again low at the deep oxycline at station 1 ( $< 1 \mu\text{M}$  for  $\text{PO}_4^{3-}$  and  $< 10 \mu\text{M}$  for TDN).  
273 In contrast high  $\text{PO}_4^{3-}$  (up to  $3.4 \mu\text{M}$ ) and high TDN (up to  $44.5 \mu\text{M}$ ) were observed in the deep OMZ at  
274 stations 2, 5 and 8 (Fig. 2d). N:P ratios were lower than the Redfield ratio (16) at all sites and depths  
275 (Fig. 2e); N:P minima were observed in surface waters (2.6 to 10 in the upper 20 m) and at  $\sim 500$  m within  
276 the core OMZ and the deep oxycline at station 1 ( $< 9$ ).

277 POC and TN concentrations ( $< 53 \mu\text{m}$  material) were highest in the euphotic zone (POC: 20 –100  
278  $\mu\text{g/L}$ ; TN: 4 – 15  $\mu\text{g/L}$ ), rapidly dropping to 5  $\mu\text{g/L}$  and 1  $\mu\text{g/L}$  below the upper OMZ, respectively (Fig.



279 3a; Suppl. Fig. 2). There were slight secondary maxima for POC (~10 µg/L) and TN (~2 µg/L) within  
280 the core of the OMZ that might reflect elevated microbial biomass there (see below). Concentrations  
281 again dropped in the deep oxycline,  $\leq 3$  µg/L and  $\leq 0.5$  µg/L for POC and TN, respectively.

282 IPL concentrations between 250 and 1500 ng/L were measured in the oxic epipelagic zone, and  
283 abruptly decreased more than 10-fold (to <20 ng/L) in the upper OMZ, following the decrease of O<sub>2</sub> levels  
284 (Fig. 3b). Secondary maxima in IPL concentrations (15 - 40 ng/L) within the OMZ at all stations roughly  
285 coincided with elevated numbers of prokaryotes (Fig. 3d). IPL/POC ratios decreased with increasing depth  
286 (Fig. 3c) and track trends of POC, TN and IPL concentrations.

287

### 288 *3.2 Changes in IPL composition with water column depth in the ETNP*

289 In total, 24 IPL classes were identified in the ETNP (Fig. 4). Based on their head group composition  
290 these were grouped into glycolipids, phospholipids or aminolipids. Figure 5 shows changes in the  
291 relative abundance of non-isoprenoidal (i.e. non-archaeal) glycolipids, phospholipids and aminolipids  
292 along the transect as well as select substitute lipid ratios (cf. Van Mooy et al., 2006; Pependorf, et al.,  
293 2011b; Carini et al., 2015). Relative abundances of phospholipids (as percentage of total measured IPLs)  
294 were highest in the core OMZ between 400 and 600 m at all sites, where they comprise up to 45-76% at  
295 stations 1, 2 and 5 and between 12 and 61% at station 8. Lower phospholipid abundances were observed  
296 within the upper OMZ and oxic zone at all stations (between 4 and 55%) and in the deep oxycline at  
297 station 8 (<1%). Aminolipid content was highest in SPM from the upper 55 m at station 5 and 8 (10 to  
298 25%), the core OMZ at station 8 (15 to 34%) and the deep oxycline at station 1 (17%). Lower aminolipid  
299 contents (2 to 11%) were observed in the oxic zone and the core OMZ at stations 1 and 2, the upper OMZ



300 at station 5 (0 to 11%) and the deep oxycline at station 8 (<2%). Glycolipid abundance was >9% at all  
301 depths, with highest abundance (average 54%, max. 82%) within the upper OMZ and oxic zone at all  
302 stations and the deep oxycline at station 8. Values down to 9% were observed within the core OMZ.

303 The phospholipid substitute ratio SQ-DAG to PG is based on the observation that cyanobacteria  
304 biosynthesize SQ-DAG preferentially over PG when phosphorus limited (Benning, 1993; Van Mooy et  
305 al., 2006, 2009) and is here for the purpose of this discussion extended to other bacteria and eukarya that  
306 are probable sources of IPLs in subsurface waters. At the ETNP this ratio ranged between 1 and 10  
307 within the upper 100-200 m along the transect and is <1 deeper into the OMZ. The ratio of DGTS to PC  
308 is reflective of the algal response to phosphorus limitation since it was observed that microalgae and some  
309 bacteria substitute PC-DAG with DGTS when phosphate concentrations are low (Van Mooy et al., 2009;  
310 Zavaleta-Pastor et al., 2010). At the ETNP this ratio did not show consistent trends and ranges between  
311 0.4 and 2.4 at most depths, but with notable spikes (>30) within the upper core OMZ at station 2 and 8, in  
312 the oxic zone at station 5 and in the lower portion of the core OMZ at station 8. Similarly, the ratio of  
313 1G-DAG to PE, which has been recently proposed to reflect the response of heterotrophic bacteria to  
314 phosphorus limitation (Carini et al., 2015) did not show any consistent trend but generally ranges between  
315 0.2 and 6 at most depths except for highly elevated values within the upper OMZ at station 2, 5 and 8 with  
316 ratios up to 800 and within the deep oxycline at station 8, where 1G-DAG:PE ratios range between 650  
317 and 950 (Fig. 5).

318

### 319 3.2.1 Major lipids

320 Major lipids are defined here as those IPL compound classes that comprised more than 10% of total





321 IPLs at more than one depth at the four stations. Eleven major IPL classes were identified. Three are  
322 assigned to an archaeal origin: 1G-GDGT, 2G-GDGT and HPH-GDGT (Suppl. Fig. 1; Fig. 4). A  
323 previous study on archaeal lipid distributions in these same ETNP samples (Xie et al., 2014) reported on  
324 only the two glycosidic archaeal IPLs (1G-GDGT and 2G-GDGT). In that study the TLE had been  
325 separated into fractions and only the glycosidic fractions had been analyzed for GDGTs. Subsequent re-  
326 examination of the original LCMS data indicate that HPH-GDGT were indeed present in an unanalyzed  
327 fraction (fraction 3 in Xie et al., 2014). The remaining eight major IPLs were assigned to either a  
328 bacterial or eukaryotic origin and were three glycolipids (1G-DAG, 2G-DAG, SQ-DAG), four  
329 phospholipids (PG-DAG, PE-DAG, PC-DAG, PE+PC-AEG) and one aminolipid (DGTS). All major  
330 lipid classes were found at all four stations and most of them occur at all depths, but with varying relative  
331 abundances (see also Suppl. Table 2).

332 *Archaeal lipids:* Relative archaeal IPL abundances generally increased with depth from non-  
333 detectable in surface waters to >50% of total IPLs at station 8 (bottom of core OMZ and deep oxycline),  
334 maximally 30% at station 1 and 2 (bottom of upper OMZ, core OMZ and deep oxycline) and generally  
335 <10% at station 5 (Fig. 4). At station 1 and 2, 1G-GDGT and 2G-GDGT were most abundant with  
336 variable amounts of HPH-GDGTs at different depths, while 1G-GDGT and HPH-GDGT dominated  
337 archaeal IPLs at station 5 and 8 at most depths. In terms of the distribution of glycosidic IPL-GDGTs  
338 these results corroborate the absolute values reported by (Xie et al., 2014) where 1G-GDGT was more  
339 abundant than 2G-GDGT at station 8 when compared to station 1.

340 *Diacylglycerol lipids:* The oxic epipelagic zone and the upper OMZ were dominated at all sites by  
341 the three diacylglycerol glycolipids, 1G-DAG, 2G-DAG and SQ-DAG, except for station 8, where the



342 sum of the three glycolipids amounted to  $\leq 50\%$  (Fig. 4). In the core OMZ and deep oxycline, relative  
343 amounts of 2G-DAG and SQ-DAG decrease, with maximal abundances of 4% and 12%, respectively. 1G-  
344 DAG amounts were lowest in the core OMZ at all stations, but increased again up to 47% of total IPL in  
345 the deep oxycline. Diacylglycerol phospholipids, PE-, PG- and PC-DAG were the second most abundant  
346 compound class group at almost all stations and depths. Average abundances of PE- and PG-DAG  
347 became highest within the upper and core OMZ, comprising over 50% in the core OMZ at station 1, >30%  
348 at stations 2 and 5, and 16% at station 8. PC-DAG did not exhibit a depth related trend and had average  
349 abundances of 5% at stations 1, 2, 8 and 3% at station 5. The third most abundant diacylglycerol class  
350 was the betaine lipid DGTS, which was present throughout the water column with average abundances of  
351 7% at station 1, 2 and 8, and 5% at station 5.

352 All of the major diacylglycerol lipids showed changes in average chain lengths and double bond  
353 numbers with depth (Fig. 6, Suppl. Table 3). The three glycolipids and PC-DAG exhibited a decrease in  
354 average length of up to three carbons and a decrease in the number of double bonds of up to 2 at the top  
355 of the upper OMZ and within the core OMZ compared to the oxic zone and the deep oxycline. Average  
356 chain length for the phospholipids PE- and PG-DAG and the betaine lipid DGTS showed an inverse profile  
357 to this, both increasing up to two carbons from the upper OMZ to the core OMZ in the average chain  
358 length. Changes in the number of double bonds were not as pronounced for PG-DAG and DGTS, but  
359 they had on average 1 to 2 double bonds more in surface waters than in deeper waters, while the number  
360 of double bonds increased on average with depth for PE-DAG.

361 *Acyl-ether glycerol lipids:* Mixed ether-ester glycerol core structures were observed with either PE  
362 or PC head groups at all stations and all depths (except for the deep oxycline at station 8) with average



363 abundances ranging between 4 and 8%.

364

### 365 3.2.2 Minor lipids

366 Minor lipids are defined as those IPL compound classes that comprised less than 10% of total IPLs  
367 at more than one depth of the four stations. In total 13 minor IPL classes were identified, five of which  
368 were glycolipids, four phospholipids and four aminolipids. All types of minor lipids could be detected  
369 at all four sites except for OH-DGTS which was not detected at Station 1. For some of these minor lipids  
370 water column stratification within the distinct zones could be observed, but some were detected at all  
371 depths (Fig. 4).

372 *Diacylglycerol lipids:* Two diacylglycerol glycolipids, 1G-OH-DAG and 3G-DAG, were detected  
373 mainly within the oxic zone and the upper OMZ, comprising between 2 to 15% of all minor lipids on  
374 average (0.1 to 0.6% of total IPLs), but also selectively reappeared within the core OMZ and deep oxycline.  
375 1G-OH-DAG showed highest relative abundances at station 5, comprising up to 40% of all minor lipids.  
376 Four phospholipids with diacylglycerol core structures were identified with the following head groups:  
377 diphosphatidylglycerol (DPG), phosphatidyl (*N*)-methylethanolamine (PME), phosphatidyl (*N,N*)-  
378 dimethylethanolamine (PDME) and phosphatidyl inositol (PI). DPG, PME-DAG and PDME-DAG had  
379 highest relative abundances (respectively 65, 56 and 35%) within the upper and core OMZ, but were also  
380 present within the oxic zone at all stations and the deep oxycline at station 1, 2 and 5. PI-DAG was most  
381 prominent in the oxic zone and the upper OMZ (up to 25%), but was also present in the core OMZ and  
382 the deep oxycline, except for station 8. Three types of aminolipids were observed as minor lipids in the  
383 ETNP. OH-DGTS with up to three hydroxyl-groups attached to the fatty acyl side chains (Suppl. Fig. 3)



384 was mainly observed at station 8 at almost all depths with an average relative abundance of 23% among  
385 the minor lipids and was selectively detected at station 2 and 5 within the oxic zone and upper OMZ.  
386 Two other aminolipids had an undefined head group that exhibited fragmentation patterns characteristic  
387 of betaine lipids, but without established betaine head group fragments (Suppl. Fig. 4b, c). The  
388 tentatively assigned sum formula for the head group of the first unknown aminolipid (AL-I) at ca. 6.7  
389 minutes LC retention time was  $C_8H_{17}NO_3$  and for the second unknown aminolipid (AL-II) at 10.5 minutes  
390 was  $C_7H_{15}NO_3$ . The head group sum formula for AL-II matches that of DGCC, however, the diagnostic  
391 head group fragment of  $m/z$  252 was not detected, and furthermore, AL-II did not elute at the expected  
392 earlier retention time for DGCC. AL-I and AL-II were detected at almost all depths at all four stations,  
393 with average abundances of 1 to 6% for AL-I and comparably higher relative abundances of AL-II ranging  
394 from 16 to 36%.

395 *Acyl-ether glycerol lipid*: One minor compound that eluted slightly earlier than SQ-DAG with a  
396 similar fragmentation pattern as SQ-DAG but with exact masses of the parent ion and MS-MS fragments  
397 in both positive and negative ion mode pointing to a mixed acyl-ether glycerol core lipid structure (Suppl.  
398 Fig. 4d, e). We therefore tentatively assigned this lipid to SQ-AEG, this IPL was observed at all four  
399 stations at almost all depths with highest relative abundances of 5 to 60% within the oxic zone.

400 *Sphingolipids*: Two types of sphingolipids were identified, monoglycosyl ceramide (1G-CER), and  
401 hydroxylated monoglycosyl ceramide (1G-OH-CER) with up to two hydroxyl groups attached to the  
402 hydrophobic side chains (Suppl Fig. 3e). Both of these lipid classes were observed at all depths at  
403 stations 1, 2, and 5 at average relative abundances between 3 and 8%, but were not detected in the deeper  
404 part of the core OMZ and the deep oxycline at station 8.



405 *Ornithine lipids*: Ornithine lipids were detected in trace amounts (<4%) in the core OMZ of station  
406 2 and 5.

407

### 408 *3.2.3 Relationships between environmental parameters and lipid distribution*

409 Spearman Rank Order Correlation was used to evaluate relationships between relative lipid  
410 abundance of lipid classes and environmental parameters (Table 1). Glycolipids 2G- and SQ-DAG  
411 showed highly significant ( $p < 0.001$ ) and positive correlations with depth, fluorescence, POC, TN,  
412 temperature and Chl- $\alpha$ , significant positive correlations were also observed with oxygen. Both  
413 glycolipids showed highly significant and negative correlations with phosphate and nitrate, and these  
414 overall trends were mirrored in the SQ-DAG:PG-DAG ratio. Total glycolipids (GL) and 1G-DAG only  
415 showed correlations with a few environmental parameters and total GL were only significantly positively  
416 correlated with oxygen. Most aminolipids and phospholipids did not show significant correlations with  
417 environmental parameters and most other correlations were neither strongly positive nor negative.  
418 Relative abundances of total aminolipids and aminolipid (AL) to phospholipid (PL) ratios correlated  
419 positively with ammonium. AL:PL also correlated positively with oxygen. Relative abundance of total  
420 phospholipids and most individual phospholipids (PG-, PE-, PME-, and PDME-DAG) correlated  
421 negatively with oxygen. The only phospholipid that significantly correlated with phosphate was PDME,  
422 however, the positive correlation is not very strong ( $r^2 < 0.4$ ).

423 NMDS analysis revealed that all samples from the oxic zone had a negative loading on the NMDS2  
424 axis along with environmental variables such as oxygen, fluorescence, TN, POC and Chl- $\alpha$ . IPLs with  
425 a strong negative loading on the NMDS2 axis (<-0.2) were 1G-OH-DAG, SQ-AEG, 2G-DAG, SQ-DAG,



426 PI-DAG and OH-DGTS. Most samples from the core OMZ and deep oxycline had a positive loading on  
427 the NMDS2 axis, together with depth, phosphate and nitrate. IPLs that showed a strong positive loading  
428 on the NMDS2 axis ( $>0.2$ ) were PDME-DAG, 2G-GDGT, DPG, PME-DAG and HPH-GDGT. Almost  
429 all environmental variables had low  $p$ -values ( $<0.001$ ), indicating highly significant fitted vectors with the  
430 exception of temperature, salinity, ammonium and nitrate. Highest goodness of fit statistic was observed  
431 with oxygen ( $r^2=0.54$ ), followed by phosphate ( $r^2=0.48$ ) and then fluorescence ( $r^2=0.46$ ).

432

#### 433 4. Discussion

434 The study area in the ETNP is characterized by moderate primary productivity in surface waters that  
435 is coupled with intense microbial degradation of particulate organic matter exported to the thermocline  
436 and restricted midwater oxygen replenishment produces the strong, shallow (~20 m deep) oxycline and a  
437 ~500 m thick OMZ with dissolved oxygen concentrations of  $<2 \mu\text{M}$ , not unlike other oceanic OMZs (e.g.,  
438 coastal upwelling off Peru and Namibia, Arabian Sea, Cariaco Basin and Black Sea; e.g. Ulloa et al.,  
439 2012). Oxygen gradients in the ETNP thus create stratified microhabitats for metazoans and microbes.  
440 Micro-grazers are critical for trophic transfer and remineralization (Sherr and Sherr, 1994) in systems like  
441 the ETNP that are dominated by picoplankton; indeed, micro-grazers in the eastern equatorial Pacific have  
442 been reported previously to consume in excess of 100% of phytoplankton production (Landry et al., 2011).  
443 During our ETNP expedition, Olsen and Daly (2013) found that micro-grazing removed 33 and 108% of  
444 surface primary production in the upper mixed layer. Peak macrozooplankton biomass was located at  
445 the thermocline, near the upper boundary of the OMZ, where food resources would be most available, but  
446 a secondary biomass peak of different zooplankton assemblage was present at the deep oxycline once  $\text{O}_2$



447 concentrations rose to  $\sim 2 \mu\text{M}$  (Wishner et al., 2013; cf. Wishner et al., 2008 for a comparable Arabian Sea  
448 investigation). Carbon and nitrogen stable isotopes in ETNP SPM (splints of the same SPM filters used  
449 for IPL analyses) and zooplankton suggest that shallow-water, plankton-derived particulate organic carbon  
450 is the primary food source for zooplankton in the mixed layer, upper oxycline and core OMZ, whereas  
451 deep POC, some of which might have been produced by microbes in the OMZ, is important for deep  
452 oxycline zooplankton (Williams et al., 2014).

453 Microbial community structure and activities in the ETNP as part of our expedition were investigated  
454 via CARD-FISH by Podlaska et al (2012). Cell numbers of total prokaryotes that are highest in the  
455 euphotic layer decreased with depth at the thermocline but rose again within the core OMZ (Fig. 2 of  
456 Podlaska et al., 2012), these are observations typical for other oxygen-deficient regions such as the  
457 upwelling area off the coast of Namibia (Woebken et al., 2007) and anoxic basins, e.g., the Black Sea and  
458 Cariaco Basin (Taylor et al., 2001; Lin et al., 2006; Wakeham et al., 2007, 2012). Bacteria dominate the  
459 prokaryotic community at all stations, but archaeal abundance can be as high as 50% and 26% at the  
460 bottom of the OMZ at stations 2 and 5, respectively. Heterotrophic activity, measured by uptake of  
461 leucine, was prevalent in and above the thermocline/upper oxycline where reactive organic matter is most  
462 available. Elevated rates of chemoautotrophy, measured by dark dissolved inorganic carbon (DIC)  
463 assimilation, were observed at several depths in the OMZ and in the lower oxycline. Dark DIC  
464 assimilation correlated with total prokaryote abundances. Mid-water microbial chemoautotrophy was  
465 further indicated by stable carbon isotope values for POC in the upper and core OMZ that are depleted by  
466 2 to 6‰ at the upper oxycline and within the OMZ compared to  $\delta^{13}\text{C}$  values of -24 to -21‰ for surface  
467 water plankton (Podlaska et al., 2009). Transfer of chemoautotrophically-fixed carbon into zooplankton



468 food webs is also evident (Williams et al., 2014). Nitrifying bacteria (nitrite-oxidizers as Nso1225-  
469 positive cells) constituted 3-7% of total DAPI-positive prokaryotes, with surface water peaks where nitrate  
470 was not detectable and in the upper OMZ where ammonium was depleted but nitrate and nitrate were high.  
471 Sulfate-reducing bacteria (SRB358-positive cells) were detected between 17 and 34% of total prokaryotes  
472 in the upper OMZ and deep oxycline where they might be associated with anoxic microzones within  
473 particle aggregates even at low dissolved oxygen concentrations (Woebken et al., 2007; Carolan et al.,  
474 2015). Similarly, anoxic microzones may be responsible for observed abundances of Planctomycetes  
475 (Pla46-positive cells; up to 24% to total prokaryotes), and anammox bacteria (Amx368-positive cells; <1%  
476 of prokaryote numbers; Podlaska et al., 2012) and ladderane lipids in the OMZ correspond with secondary  
477 nitrite maxima. Nitrate deficits point to nitrate reduction as a source for nitrite in the OMZ. Archaeal  
478 cell abundances peak at the start of the upper OMZ at all stations (reaching maximal values of 37% of  
479 total prokaryotes at station 2), within the core OMZ at station 2 (up to 54% of total detected cells at station  
480 2) and within the deep oxycline at station 5 and 8 (around 25%; Fig. 2e). These peaks in archaeal cells  
481 are further corroborated by maxima in 1G- and 2G-GDGT abundances at 120 m and 725 m at station 1  
482 and at 200 m and 550 m at station 8 reported by (Xie et al., 2014). Crenarchaeota and thaumarchaeota  
483 (as Cren537-positive cells) represented ~20% of prokaryotes throughout the water column, generally  
484 being highest in the lower OMZ and deep oxycline, and at stations 2 and 5 just above the secondary Chl-  
485 *a* maxima at ~75 m. Euryarchaeota (Eury806-positive cells) were 16-20% of total prokaryotes,  
486 especially in waters above the OMZ, and generally correlating with ammonium concentrations and  
487 heterotrophic potential.

488 Total IPL concentrations that were over 50 times higher in the surface waters than at deeper depths





489 coincide with high Chl- $\alpha$  concentrations reflecting the importance of eukaryotic rather than microbial  
490 sources to the IPL pool above the thermocline. Below the thermocline, IPL concentrations generally  
491 track trends observed in the cell abundances, with elevated IPL concentrations in the upper and core OMZ  
492 whenever nitrite concentrations are elevated. The rapid decrease in IPL concentrations below ~100 m  
493 probably results from a combination of a dearth of potential source organisms and the decomposition of  
494 detrital lipids (Harvey et al., 1986; Matos and Pham-Thi, 2009) associated with particulate matter sinking  
495 from above. Substantial IPL concentration decreases below the euphotic zone have been observed  
496 elsewhere (Van Mooy et al., 2006; Schubotz et al., 2009; Van Mooy and Fredricks, 2010; Popendorf et al.,  
497 2011b; Wakeham et al., 2012). Despite these low absolute concentrations of IPL, the diversity of  
498 molecular compositions and significant changes in relative abundances of IPLs reflect a complex  
499 eukaryotic and prokaryotic community structure throughout the water column of the ETNP.

500

#### 501 *4.1 Sources for IPLs in the water column of the ETNP*

502 Distinct changes in IPL relative abundances and core lipid compositions coincide with the  
503 biogeochemical zonation of the OMZ at all four stations, although many of the IPL were detected at  
504 multiple depths. Potential sources and possible physiological roles for the observed IPLs in the different  
505 zones are discussed below.

506

##### 507 *4.1.1 Oxidic zone*

508 The glycosyldiacylglycerides that dominate the IPL composition in surface waters, 1G-DAG, 2G-  
509 DAG and SQ-DAG, are major constituents of photosynthetic thylakoid and chloroplast membranes of



510 plants (Poincelot 1973, Mackender and Leech, 1974; Nishihara et al., 1980), eukaryotic algae (Araki et  
511 al., 1991; Thompson, 1996) and cyanobacteria (Wada and Murata, 1998; Siegenthaler, 1998). They are  
512 commonly the most abundant IPLs in oceanic surface waters (Van Mooy et al., 2006; Schubotz et al.,  
513 2009; Van Mooy and Fredricks, 2010; Pependorf et al., 2011b; Wakeham et al., 2012), where they are  
514 assigned to photosynthetic algae or cyanobacteria. The acyl groups of the glycolipids can give further  
515 indications about their biologic sources. 1G- and 2G-DAG are dominated by C<sub>16</sub> and C<sub>18</sub> fatty acids in the  
516 euphotic zone with zero to 4 double bonds (Suppl. Table 1, Fig. 6). Many different combinations of  
517 polyunsaturated fatty acids (PUFA) are observed, such as C<sub>16:4</sub>/C<sub>18:3</sub>, C<sub>16:4</sub>/C<sub>18:4</sub>, C<sub>18:3</sub>/C<sub>16:2</sub>, C<sub>18:4</sub>/C<sub>14:0</sub> and  
518 C<sub>18:5</sub>/C<sub>14:0</sub>, which are characteristic for marine phytoplankton (Brett and Müller-Navarra, 1997; Okuyama  
519 et al., 1993). SQ-DAG in the ETNP do not contain these PUFA, but instead have predominantly  
520 combinations of C<sub>14:0</sub>, C<sub>16:0</sub>, and C<sub>16:1</sub> fatty acids, resulting in shorter chain lengths and a lower average  
521 number of double bonds (0.5 to 1) than the other glycolipids in surface waters (Fig. 6). This is consistent  
522 with SQ-DAG being primarily derived from marine cyanobacteria that mainly have saturated and  
523 monounsaturated C<sub>14</sub> and C<sub>16</sub> fatty acids (e.g., Siegenthaler, 1998). Cyanobacteria are therefore likely  
524 the primary source organisms for all three glycolipids in the euphotic zone and upper OMZ of the ETNP  
525 as they were abundant from the surface waters into the upper OMZ (as indicated by divinyl chlorophyll  $\alpha$ ,  
526 a diagnostic pigment for *Prochlorococcus* cyanobacteria, Suppl. Table 1; see also Goericke et al., 2000;  
527 Ma et al., 2009), notably at the secondary fluorescence maxima that were observed just below the  
528 thermocline, especially at stations 1 and 8. The PUFA fatty acids in 1G-DAG and 2G-DAG additionally  
529 indicate mixtures of eukaryotic algae as source for these lipids. The presence of eukaryotic algae, such  
530 as diatoms (characteristic pigment: 19'hexanoyloxyfucoxanthin) and Prymnesiophytes (characteristic



531 pigment: 19'butanoyloxyfucoxanthin; Suppl. Table 1) albeit not as abundant as cyanobacteria, is also  
532 indicated by the detection of PC-DAG with fatty acyl combinations of C<sub>22:6</sub> and C<sub>20:5</sub> long chain PUFA  
533 and C<sub>16:0</sub> fatty acids (Suppl. Table 3). These long chain PUFAs are common in many eukaryotic  
534 phytoplankton (Brett and Müller-Navarra, 1997; Okuyama et al., 1993). Stable carbon isotope labeling  
535 experiments in the North Atlantic have confirmed the importance of a phytoplankton source for PC in  
536 surface waters (Popendorf et al., 2011a). Betaine lipids such as DGTS, which are also diagnostic  
537 eukaryotic algal markers (Dembitsky, 1996; Popendorf et al., 2011a), are present in surface waters of the  
538 ETNP in abundances similar to those of PC. Major acyl moieties of betaine lipids were C<sub>14</sub>, C<sub>16</sub>, C<sub>18</sub> and  
539 C<sub>20</sub> with multiple unsaturations (on average 1.5 to 3 double bonds).

540 Eukaryotic phytoplankton and cyanobacteria are assumed to be a major source for PG-DAG in the  
541 euphotic zone as it is the only phospholipid in cyanobacteria and thylakoid membranes (Wada and Murata,  
542 1998). Popendorf et al. (2011a) have shown that in surface waters of the Atlantic heterotrophic bacteria  
543 seem to be a dominant source for PG-DAG, which is consistent with it being a major phospholipid in  
544 bacterial membranes (Goldfine, 1984). Similarly, PE-DAG is a common phospholipid in membranes of  
545 bacteria (Oliver and Colwell, 1973; Goldfine, 1984) and is also sometimes present in low abundances in  
546 eukaryotic algae (e.g., Dembitsky et al., 1996). Both of these sources have been confirmed for PE-DAG  
547 in surface waters of the Atlantic (Popendorf et al., 2011a). We therefore suggest heterotrophic bacteria  
548 to be the major source for PE and PG-DAG in the euphotic zone of the ETNP, with cyanobacteria being  
549 responsible for PG-DAG and heterotrophic bacteria for PE-DAG. Lower average number of double  
550 bonds in PG and PE-DAG (<2) is consistent with a primarily bacterially-derived source of these lipids in  
551 the upper water column of the ETNP (Fig. 6).



552 PE and PC also occurred with mixed acyl and ether lipids (AEG) in their core structures. PE-AEG  
553 have been described in some sulfate-reducing bacteria (Rütters et al., 2001), which are, however, an  
554 unlikely source in the oxic water column of the ETNP, unless in anoxic microzones of fecal pellets or  
555 aggregates (e.g., Bianchi et al., 1992; Shanks and Reeder, 1993). A recent study of surface waters of the  
556 Southern Ocean and the eastern South Atlantic Ocean found increased abundances of 1-*O*-monoalkyl  
557 glycerol ethers (MAGE), which are presumably breakdown products of PE- and PC-AEGs (Hernandez-  
558 Sanchez et al., 2014). These authors suggested aerobic bacteria to be a likely source for these lipids, but  
559 cultured representatives are currently lacking to confirm this conclusion. The relative abundance of  
560 MAGE-based phospholipids, 4 to 7% of total IPLs, although low, highlights the overall significance of  
561 these orphan lipids in the surface waters of the ETNP. Similarly, some of the observed minor IPL  
562 compounds have to date not been described in culture, including SQ-AEG. Since SQ is a diagnostic  
563 headgroup found in cyanobacteria, we suggest that cyanobacteria are a likely source for SQ-AEG in the  
564 ETNP surface waters, although, again, these lipids have not been reported in cultured cyanobacteria.  
565 3G-DAG, another minor IPL detected in the euphotic zone at all stations except for station 5 with up to  
566 six double bonds and C<sub>14</sub>, C<sub>16</sub> and C<sub>18</sub> fatty acid has been found in some plants (Hölzl and Dörmann, 2007)  
567 and some anaerobic gram-positive bacteria (Exterkate and Veerkamp, 1969). We thus propose that  
568 eukaryotic algae are the probable source for this glycolipid in the euphotic zone of the ETNP.  
569 Phospholipids detected in minor amounts in the euphotic zone include PI-DAG and DPG. As these are  
570 also minor components in several types of marine algae (Dembitsky, 1996) and bacteria (Morita et al.,  
571 2010; Diervo et al., 1975; Mileykovskaya and Dowhan, 2009), mixed inputs are likely for these IPLs.  
572 Likewise, bacteria in the oxic euphotic zone may be the origin of the low detected levels of *N*-methylated



573 phospholipids (Goldfine and Ellis, 1964).

574 1G-CER belongs to the class of sphingolipids consisting of a sphingosine backbone linked to a fatty  
575 acid via an amide bond. 1G-CER was detected in the oxic zone as a minor component with relative  
576 abundance less than 5% of IPL at all stations (Fig. 4). Glycosidic ceramides occur in eukaryotic algae  
577 such as the coccolithophore *Emiliana huxleyi* (Vardi et al., 2009). We also detected 1G-OH-CER with  
578 up to 2 hydroxylations in the core lipid structure (Suppl. Fig. 3). The presence of multiple-hydroxylated  
579 sphingoid bases has been proposed as a marker for viral infection and cell death in at least some marine  
580 phytoplankton, such as *Emiliana huxleyi* in the study of Vardi et al. (2009). We did not, however, find  
581 mass spectral evidence for the presence of viral polyhydroxylated 1G-CER, as described by Vardi et al.  
582 (2009) and therefore rather suggest that eukaryotic algal cells are potential sources for the G-CER (Lynch  
583 and Dunn et al., 2004) in surface waters of the ETNP. Apart from the presence of hydroxylated  
584 sphingolipids, a notable observation was the presence of hydroxylated glycolipids (1G-OH-DAG) and  
585 aminolipids (OH-DGTS) with up to two hydroxyl-groups or one hydroxyl group combined with an epoxy  
586 or keto function attached to the fatty acyl groups (Suppl. Fig. 3). The addition of hydroxyl groups or  
587 general oxygenation of fatty acids in plants, algae and yeast has been identified as a defense mechanism  
588 and response to oxidative stress (Kato et al., 1984; Andreou et al., 2009). Hydroxy fatty acids, for  
589 example, are intermediates in oxidative degradation of fatty acids (Lehninger, 1970), and since they are  
590 constituents of structural biopolymers of many microorganisms (Ratledge and Wilkinson, 1988), they are  
591 present in marine particulate matter (e.g., Wakeham, 1999), derived from membrane constituents of Gram  
592 negative bacteria, the most abundant bacteria in seawater (Rappé and Giovannoni, 2000).

593



## 594 4.1.2 Upper OMZ

595 Within the upper OMZ below the thermocline/oxycline, glycolipid abundance varied between 15 to  
596 80% of total IPL, but notably SQ-DAG and 2G-DAG exhibited strong decreases in relative and absolute  
597 abundance below 125 m at all stations consistent with the decrease in phytoplankton biomass as seen in  
598 Chl- $\alpha$  profiles. Anoxygenic phototrophic bacteria might be a source of these glycolipids (Hölzl and  
599 Dörmann, 2007) in the upper OMZ, which overlapped with the base of the euphotic zone. Other  
600 anaerobic bacteria, including sulfate-reducing bacteria, are able to replace phospholipids with glycolipids,  
601 particularly 1G-DAG, when phosphate concentrations were  $<20 \mu\text{M}$  (Bosak et al., 2016). Sulfate-  
602 reducing bacteria ( $\delta$ -proteobacteria) comprised up to 10% of the total bacterial communities in the upper  
603 OMZ (Podlaska et al., 2012). Other  $\alpha$ -,  $\beta$ -,  $\gamma$ -,  $\epsilon$ -proteobacteria were also abundant in the upper OMZ.  
604 Since aerobic representatives of these classes are capable of similar phospholipid substitutions (Geske et  
605 al., 2012; Carini et al., 2015; Sebastian et al., 2016; Yao et al., 2015), we infer that the presence of  
606 1G-DAG could indicate P-limited proteobacteria within the upper OMZ, considering phosphate levels in  
607 the upper OMZ of the ETNP range between 2 to  $2.5 \mu\text{M}$ . Notably, relative glycolipid abundance was  
608 very high within the upper OMZ, while phospholipid abundance was low (Figs. 2, 4), particularly at station  
609 2 and 5 where glycolipids comprise  $>80\%$  of total IPLs. Core lipid chain length and number of double  
610 bonds of all three glycolipids showed considerable variations within the upper OMZ (Fig. 6), indicating a  
611 change in source organisms compared to the oxic zone. Both PC-DAG and DGTS decreased in chain  
612 length and number of double bonds at most stations within the upper OMZ and became increasingly  
613 dominated by  $\text{C}_{14}$ ,  $\text{C}_{16}$  and  $\text{C}_{18}$  saturated and monounsaturated fatty acids (Suppl. Table 3). This likely  
614 reflects a change from eukaryotic to bacterial sources for these IPLs. Similar to 1G-DAG, DGTS can



615 function as a substitute lipid under phosphorus limitation in some bacteria (Geiger et al., 1999; Sebastian  
616 et al., 2016) and we thus suggest that phosphate concentrations around 2  $\mu\text{M}$  induce such ecological  
617 changes in the water column of the ETNP. AL-I and AL-II are other non-phosphorus-containing IPL  
618 that remain abundant within the minor IPLs in the upper OMZ. Since we could not elucidate the structure  
619 of these lipids (Supp. Fig. 4) potential bacterial source(s) remain unclear. Phospholipids PME- and  
620 PDME-DAG and DPG increase in abundance within the upper OMZ and indicate an increased abundance  
621 of bacteria at these depths, as has been observed in other stratified water bodies (Schubotz et al., 2009;  
622 Wakeham et al., 2012).

623 G-CER and 1G-OH-CER were detected in the upper OMZ in similar relative amounts as in the oxic  
624 zone but microbial sources for these IPLs in suboxic environments remain unclear. Their abundant  
625 presence in the anoxic zones of the stratified Black Sea (Schubotz et al., 2009) and Cariaco Basin  
626 (Wakeham et al., 2012) has been previously assigned to as yet unidentified anaerobic bacteria. The  
627 oxygenated glycolipids and betaine lipids that were observed in the oxic zone are also present within the  
628 upper OMZ at most of the stations and thus underline a likely bacterial source of these currently  
629 unassigned IPLs and potentially signify oxidative stress or other acting defense mechanisms, (cf. Kato et  
630 al., 1984; Andreou et al., 2009).

631 Archaeal IPLs with glycosidic headgroups and tetraether core structures (1G- and 2G-GDGT) were a  
632 greater proportion of the overall IPL pool within the upper OMZ. As shown by Xie et al. (2014) in an  
633 earlier analysis of these same samples, absolute abundances of glycosidic GDGTs peak roughly at depths  
634 where nitrite maxima are observed, consistent with the source archaea being ammonium oxidizers,  
635 comparable to other OMZs around the world (e.g., Pitcher et al., 2011; Schouten et al., 2012). At all



636 stations GDGTs with hexose-phosphate-hexose (HPH) headgroups were observed at depths of nitrate  
637 maxima, but at deeper depths as well. HPH headgroups are common among ammonium oxidizing t  
638 haumarchaeota (Elling et al., 2017). Other archaeal sources such as Marine Group II euryarchaeota  
639 (Zhu et al., 2016; Lincoln et al., 2014), are possible for the observed glycosidic GDGTs, since Podlaska  
640 et al. (2012) detected both crenarchaeota/thaumarchaeota and euryarchaeota within the upper OMZ of the  
641 ETNP.

642

#### 643 *4.1.3 Core OMZ and deep oxycline*

644 IPL distributions in the core OMZ and at the deep oxycline of the ETNP were notably different from  
645 the oxic zone and the upper OMZ. In general, phospholipid abundance increased at all stations to over  
646 50% (except for station 8) while glycolipid abundance decreased. Chain length and number of double  
647 bonds were distinctly different within the core OMZ compared to the overlying water column (Fig. 6).  
648 For instance, the PUFA that were observed in the euphotic zone and that are widespread in marine  
649 phytoplankton (Brett and Müller-Navarra, 1997; Okuyama et al., 1993) became less abundant at the deeper  
650 depths (Suppl. Table 3), indicating either the decline of sources or rapid degradation of these labile, highly  
651 unsaturated compounds (De Baar et al., 1983; Prahl et al., 1984, Neal et al., 1986). Degradation is the  
652 more likely scenario since marine bacteria, including deep-sea species, are capable of biosynthesizing  
653 PUFAs (DeLong and Yayanos, 1986, Fang et al. 2003; Valentine and Valentine, 2004). PE and PG-DAG  
654 were the most abundant phospholipids in the core OMZ, followed by PC-DAG and PE- and PC-AEG.  
655 We interpret the increase in phospholipid abundance as due to the increase in bacterial abundance within  
656 the OMZ. This is also reinforced by the increase of DPG, PME and PDME-DAG among the minor lipids





657 (Fig. 4). Multiple bacterial sources are possible since PE, PG and DPG are common phospholipids in  
658 membranes of most proteobacteria (Oliver and Colwell, 1973; Goldfine, 1984), and genes for the synthesis  
659 of PME, PDME and PC are widespread among  $\alpha$ -,  $\gamma$ - and some  $\beta$ -proteobacteria, all of which were  
660 abundant within the core OMZ and deep oxycline (20 to 40% of the total bacterial population, Podlaska  
661 et al., 2012). Fatty acid combinations for the detected phospholipids included saturated  $C_{14:0}$ ,  $C_{15:0}$  and  
662  $C_{16:0}$  and monounsaturated  $C_{16:0}$ ,  $C_{17}$  and  $C_{18:0}$  (Suppl. Table 3). The increased proportion of odd-chain  
663 fatty acids further underpins a bacterial origin for these phospholipids.

664 The three glycolipids that dominate surface water IPLs were also present in the core OMZ and most  
665 parts of the deep oxycline, although at greatly reduced concentrations. Since chain length and number  
666 of double bonds were distinct from the surface waters, with on average 1 to 2 carbon atoms shorter chain  
667 lengths and 1 to 3 fewer double bonds at all sites (Fig. 6), we infer a microbial source for these glycolipids  
668 within the OMZ. In the core OMZ and deep oxycline SQ-DAG with combinations of fatty acids with  
669 odd numbers of carbon atoms (e.g.,  $C_{15:0}/C_{16:0}$  and  $C_{14:0}/C_{15:0}$ ) further support a bacterial source for this  
670 IPL, despite its widespread attribution as cyanobacterial marker in environmental studies. Indeed, SQ-,  
671 1G- and 2G-DAG have been reported in some members of the Gram-positive *Bacillus* and *Firmicutes*  
672 (Hölzl and Dörmann, 2007) and their presence in deeply buried Wadden Sea sediments has been ascribed  
673 to an anaerobic bacterial source (Seidel et al., 2012). Unfortunately, Gram-positive bacteria were not  
674 specifically targeted in previous phylogenetic characterizations of the OMZ of the ETNP (Podlaska et al.,  
675 2012). However, in the OMZ of the eastern tropical South Pacific Gram-positive bacteria such as  
676 *Actinobacteria* accounted only for a negligible amount of total prokaryotic community (Stevens and Ulloa,  
677 2008) and are thus likely not contributing significantly to the glycolipids in the core OMZ.



678 Aminolipids, DGTS and betaine lipid like AL-II, were observed in similar relative abundances in the  
679 core OMZ and deep oxycline as in the overlying shallower water column. The presence of DGTS has  
680 so far only been reported in a few aerobic proteobacteria, and then only when grown under phosphorus  
681 limitation (Benning et al., 1993; Geiger et al., 1999; Sebastian et al., 2016). Consequently, potential  
682 bacterial sources for the aminolipids in the core OMZ remain elusive, particularly since these regions are  
683 not considered to be phosphorus limited with phosphate concentrations exceeding several micromolar (Fig.  
684 2).

685 Bacterial sources for 1G-CER and 1G-OH-CER within the core OMZ and deep oxycline remain  
686 similarly unresolved, but as suggested for anoxic water columns (Schubotz et al., 2009; Wakeham et al.,  
687 2012), uncultured anaerobic bacteria are potential source organisms. Ornithine lipids, also non-  
688 phosphorus containing lipids but which are not known to play important roles in lipid substitutions (cf.  
689 Geiger et al., 2010), were present in minor to trace amounts within the core OMZ and can be assigned to  
690 Gram-negative bacteria.

691 For several of the major IPLs, such as 2G-DAG, PC-DAG and DGTS, the average chain length and  
692 number of double bonds increased again to levels observed in surface waters within the deep oxycline  
693 layer (Fig. 6). PC-DAG and DGTS both contained long-chain PUFA, specifically in the case of DGTS  
694 and 2G-DAG, C<sub>16:4</sub> and C<sub>18:3</sub>. This could thus reflect an exported fossil signal from the surface water,  
695 however, since experimental studies of IPL degradation, including PC, have not provided evidence for  
696 selective preservation of phospholipids (Logemann et al., 2011), we exclude the possibility that the  
697 presence of PUFAs represents a fossil signal exported from the surface waters but rather propose a deep-  
698 sea bacterial source (DeLong and Yayanos, 1986; Fang et al. 2003; Valentine and Valentine, 2004), as



699 noted above.

700 Head group variations of GDGTs in the core OMZ/deep oxycline depth region were similar to their  
701 distributions in the upper OMZ, with a notable increase of HPH-GDGTs with depth at stations 2 and 5.  
702 Similar to the upper OMZ, archaeal sources for the detected IPL-GDGTs could be either euryarchaeota,  
703 crenarchaeota or thaumarchaeota (Lincoln et al., 2014; Elling et al., 2017) as these phyla were detected  
704 within the core OMZ and deep oxycline of the ETNP (Podlaska et al., 2012). Relative archaeal IPL  
705 abundances within the core OMZ and deep oxycline vary between stations, but were highest at station 8  
706 where they reach over 50% of the total microbial IPLs. Elevated abundances of archaea had been  
707 enumerated by quantification via CARD-FISH (Podlaska et al., 2012), with highest abundances (25 to 50%  
708 of total DAPI-stained cells) at stations 2 and 5. It should be noted again, however, that >50% of the  
709 microbial populations that were DAPI-positive cells remained uncharacterized by the CARD-FISH  
710 approach used (Suppl. Fig. 2).

711

#### 712 *4.2 Factors influencing IPL distribution*

713 Relative abundances of IPLs in the oxic zone of the ETNP were distinct from IPL distributions in  
714 surface waters of other oceanic ocean regions where SQ-DAG and PC-DAG were typically the most  
715 abundant compounds within the glycolipids and phospholipids, respectively (Van Mooy and Fredricks,  
716 2010; Pependorf et al., 2011a,b). Whereas SQ-DAG was among the most abundant IPL in the surface  
717 waters of the ETNP (18-50%), PC-DAG was comparably minor (3-13%). This difference might result  
718 from the highly compressed mixed layer of the ETNP compared to other locales, with consequent  
719 differences in plankton ecology. Alternatively, there could be differences in physiologic adaptations and



720 hence membrane lipid modifications between the ETNP and other regions, (e.g., Van Mooy et al., 2009).  
721 In general, our study confirms the dominance of glycolipids as a common feature of surface ocean waters  
722 in which IPL distributions have been determined, in particular the Black Sea (Schubotz et al., 2009), the  
723 Eastern Subtropical South Pacific (Van Mooy and Fredricks, 2010), the Western North Atlantic  
724 (Popendorf et al., 2011a), the Mediterranean Sea (Popendorf et al., 2011b) and the Cariaco Basin  
725 (Wakeham et al., 2012). In addition, the present study highlights the potential importance of glycolipids  
726 and other non-phosphorus lipids for bacteria in low oxygen environments as will be discussed in detail  
727 below.

728

#### 729 *4.2.1 Influence of environmental parameters on IPL distribution*

730 The NMDS analyses and Spearman Rank Order Correlations provide a better understanding of the  
731 influence of environmental factors and the microbial community structure on the IPL composition in the  
732 water column of the ETNP. NMDS analysis of normalized IPL composition and quantitative microbial  
733 data (abundance of  $\alpha$ ,  $\beta$ ,  $\gamma$ ,  $\epsilon$ -proteobacteria, sulfate-reducing bacteria  $\delta$ -proteobacteria, planctomycetes,  
734 crenarchaeota including thaumarchaeote and euryarchaeota) did not yield any high goodness of fit statistic  
735 ( $r^2 < 0.3$ ; Suppl. Table 4). There are several potential reasons for this, the most likely being that IPL also  
736 derive from eukaryotes in the oxic zone and secondly because many of the proteobacteria in fact also  
737 biosynthesize similar IPL assemblages. Changes in bacterial community structure might not necessarily  
738 result in significant variations in IPL composition. Rather than focusing solely on IPL source, we were  
739 interested in deciphering whether environmental factors such as temperature, nutrient or oxygen  
740 concentrations might affect IPL composition and thus compare any environmental impact with what has



741 been observed in culture studies and other natural settings. Many of the major and minor glycolipids  
742 were loaded negatively on the NMDS2 axis, as were oxygen, fluorescence, Chl- $\alpha$ , POC and TN, with the  
743 notable exception of 1G-DAG which had only a slightly negative loading on the NMDS-2 axis. These  
744 relationships (loadings) roughly reflect the vertical distribution of IPLs in the water column of the ETNP.  
745 Glycolipids, particularly 2G-DAG and SQ-DAG, were most abundant in the oxic zone characterized by  
746 high oxygen concentration and moderate primary productivity (high POC, TN and elevated Chl- $\alpha$  and  
747 fluorescence). Spearman Rank Order Correlations confirm these observations, including the lack of  
748 significant correlations between 1G-DAG and depth or any other environmental parameter. One  
749 explanation for this is that 1G-DAG has diverse sources throughout the water column independent of any  
750 environmental variable. Phospholipids, and in particular PE-, PME- and PDME-DAG, become more  
751 prevalent within the core OMZ where eukaryotic sources were minimal and non-photosynthetic bacteria  
752 dominated the microbial communities and at deeper depths where nutrient concentrations ( $\text{NO}_3^-$  and  $\text{PO}_4^{3-}$ )  
753 were elevated due to organic matter remineralization, giving positive loadings of these environmental  
754 parameters on the NDMS2 axis. Notably only the minor phospholipids, DPG, PME-, and PDME-DAG,  
755 showed a similar positive loading on the NDMS2 axis as did depth,  $\text{NO}_3^-$  and  $\text{PO}_4^{3-}$ . Most major  
756 phospholipids and aminolipids did not correlate with any of the tested environmental variables, due to  
757 their presence in equal relative abundances within all the different biogeochemical zones. This is also  
758 reflected in the lack of Spearman Rank Order Correlation for most of the major lipids with environmental  
759 parameters (Table 1). In contrast, most archaeal IPLs showed a positive loading on the NMDS2 axis,  
760 consistent with the increasing importance of archaeal abundance with depth and at reduced oxygen  
761 concentrations.



762

763 *4.2.2 Links between substitute lipid ratios and nutrient concentrations*

764 Because they have similar biochemical functions and the same ionic charge at physiological pH,  
765 SQ-DAG and DGTS are known as substitute lipids for PG-DAG and PC-DAG, respectively, when  
766 phosphorus is limiting (Benning et al., 1993; Van Mooy et al., 2009; Popendorf et al., 2011b). The  
767 elevated ratios of SQ-DAG:PG-DAG and DGTS:PC-DAG in the surface waters of phosphorus-limited  
768 Sargasso Sea (4 to 13) compared to phosphorus-replete South Pacific (3) suggests that phytoplankton  
769 synthesize phosphorus-free substitute lipids to maintain growth in response to phosphorus starvation (Van  
770 Mooy et al., 2009). Underlining this observation, relative abundance of phospholipids was positively  
771 correlated with phosphate concentration across the Mediterranean Sea (Popendorf et al., 2011b).  
772 Microcosm incubations of seawater from the Mediterranean Sea supplemented with phosphate and  
773 ammonium confirmed that changes in substitute lipid ratios were partly caused by a physiological  
774 response to nutrients (Popendorf et al., 2011b). However, neither of these substitute lipid ratios was  
775 significantly correlated with abundance of phosphate in surface waters of the Eastern Subtropical South  
776 Pacific (Van Mooy and Fredericks, 2010), leading the authors to conclude that not only phosphate  
777 limitation but also algal community structure may impact these ratios.

778 To further explore the possibility that SQ-DAG and aminolipids (DGTS) in the OMZ of the ETNP  
779 might serve as substitute lipids, we performed a Spearman Rank Order Correlation of known substitute  
780 lipid ratios as well as total aminolipid (AL) to phospholipid (PL) and total glycolipid (GL) to PL ratios  
781 with nutrient concentrations and other environmental parameters. Only SQ-DAG:PG-DAG was  
782 significantly correlated with phosphate (-0.56,  $p < 0.001$ ) but also correlated with other parameters, such



783 as depth ( $-0.76$ ,  $p < 0.001$ ) and oxygen concentration ( $0.58$ ,  $p < 0.001$ ). These correlations reflect the  
784 elevated SQ-DAG:PG-DAG ratios ( $>2$ ) in the surface waters and upper OMZ (Fig. 4) and support the  
785 notion that SQ-DAG functions as a substitute lipid in the ETNP where phosphate concentrations are  $<2$   
786  $\mu\text{M}$ . The other proposed substitute lipid ratios, DGTS:PC-DAG (Van Mooy et al., 2009) and  
787 1G-DAG:PE-DAG (Carini et al., 2015), did not correlate with nutrient concentrations in the water column  
788 of the ETNP but rather showed highly variable distributions. Similarly, AL:PL ratios did not exhibit  
789 strong relationships with any environmental parameter, and GL:PL ratios showed similar but less  
790 pronounced trends as SQ-DAG:PG-DAG ratios. Similar to the suggestion of Van Mooy and Fredericks  
791 (2010) for the Eastern Subtropical South Pacific, the lack of a correlation of these substitute lipid ratios  
792 with phosphorus in the ETNP might be due to changes in community composition and not to phosphorus  
793 limitation, since phosphate concentrations increase within the core OMZ and the deep oxycline.  
794 However, this interpretation stands in contrast to what is currently known from cultured representatives,  
795 that replace their phospholipid content with glycolipids at phosphate concentrations  $<20 \mu\text{M}$  (e.g., Bosak  
796 et al., 2016). Accordingly, many of the organisms living within the OMZ may already be phosphorus  
797 limited at micromolar concentrations of phosphate.

798

#### 799 *4.2.3 Factors affecting structural diversity of the core lipid composition*

800 We observed a considerable diversity in both headgroup and core lipid types, from diacylglycerol  
801 lipids with varying chain lengths and zero to multiple unsaturations, with or without hydroxylations to  
802 mixed ether/ester glycerolipids, sphingolipids and ornithine lipids. Changes in core lipid chain length or  
803 unsaturations are often associated with temperature. However, NMDS analysis did not yield any strong



804 correlations with temperature and chain length or number of double bonds of the major IPL classes ( $r^2 <$   
805  $0.02$ , Suppl. Table 4), or with other environmental parameters ( $r^2 < 0.3$ , Suppl. Table 4). Instead, we  
806 conclude that observed changes in chain length and unsaturations are most likely due to changing  
807 biological sources. For instance, long chain PUFAs in surface waters are mainly synthesized by  
808 phytoplankton, while in deeper waters myriad bacterial sources are probable. Likewise, hydroxylations  
809 in the acyl side chains did not show any clear link to specific environmental factors, although, both  
810 1G-OH-Cer and OH-DGTS showed negative loadings on the NMDS-2 axis indicating a higher abundance  
811 of these compounds in oxic samples. This is in accordance with the previous assumption that these lipids  
812 play a role during oxidative stress and/or are involved in other defense mechanisms. The occurrence of  
813 mixed ether-acyl lipids in ocean waters has been reported previously in a wide number of oceanic settings  
814 (Hernandez-Sanchez et al., 2014) where aerobic bacteria were suggested as source organisms. In our  
815 study we detected PE- and PC-AEG at all depths in the ETNP but with no noticeable correlation with  
816 depth or oxygen concentrations (Fig. 7) and thus we suggest that various bacteria living in both the  
817 oxygenated surface waters and in the suboxic OMZ are potential sources for these compounds in the water  
818 column.

819 Ornithine lipids and sphingolipids play many functional roles in biological systems, confounding  
820 identification of potential sources. Ornithine lipids were strongly negatively loaded on the NMDS-1 axis,  
821 but none of the measured environmental parameters could account for this negative loading (Fig. 7).  
822 Therefore, it remains unclear what factor(s) ultimately determine their distribution. Likewise, the  
823 absence of significant correlations between the sphingolipid 1G-Cer, and any environmental parameter  
824 lead us to conclude that the abundance of 1G-Cer reflects the diverse microbes inhabiting the changing





825 oxygen regime within the water column rather than any specific source organism.

826

## 827 **5. Conclusions**

828 Diverse intact polar lipids, including four classes of diacylglycerol glycolipids (with monoglycosyl,  
829 diglycosyl, triglycosyl and sulfoquinovosyl head groups), seven diacylglycerol phospholipids (with  
830 phosphatidyl glycerol, phosphatidyl ethanolamine, phosphatidyl choline, phosphatidyl (*N*)-  
831 methylethanolamine, phosphatidyl (*N,N*)-dimethylethanolamine, diphosphatidyl glycerol and  
832 phosphatidyl inositol head groups) and three diacylglycerol aminolipids (with homoserine and two  
833 unidentified head groups) are present in the water column of the ETNP. Mixed ester-ether glycerol lipids  
834 with phosphatidyl ethanolamine, phosphatidyl choline and sulfoquinovosyl head groups as well as  
835 glycosidic ceramides and ornithine lipids were detected throughout the water column. A wide range of  
836 archaeal GDGTs were most abundant within the OMZ. This diversity in IPL compositions reflects the  
837 dynamic nature of the biological community that inhabits the range of environments in the ETNP, with  
838 oxygen as a primary determinant, from fully oxygenated surface waters to a strong oxygen minimum zone  
839 at depth. Highest concentrations of IPLs (250 – 1500 ng/L) in oxygenated surface waters zone reflect  
840 the dominance of phototrophic eukaryotic and cyanobacterial sources above the OMZ, but secondary  
841 peaks in IPL concentration (12 – 56 ng/L) within the core of the OMZ result from elevated abundances of  
842 heterotrophic and chemoautotrophic bacteria and archaea under low oxygen conditions. Glycolipids  
843 derived from photoautotrophs generally accounted for more than 50% of total IPLs in the euphotic zone  
844 (< 200 m, oxic and upper OMZ zones), while bacterial phospholipids were more predominant (avg. 40%)  
845 in the OMZ and deep oxycline layers. Depth-related variations in the dominant fatty acid compositions



846 for each IPL class show that specific biological source(s) for each IPL were distinct in each depth/oxygen-  
847 content horizon. Nevertheless, microbial sources for many of the detected lipids remain unclear and  
848 therefore potentially unique ecophysiological adaptations these lipids may represent remain to be explored.  
849 The presence of the glycolipid, monoglycosyl diacylglycerol (1G-DAG), and the betaine lipid,  
850 diacylglyceryl homoserine (DGTS), with varying fatty acid compositions, within all zones indicates that  
851 these canonical phototrophic markers may indeed be synthesized in different parts of the water column by  
852 a much larger host of organisms (including non-phototrophs) than previously thought. Since 1G-DAG  
853 and DGTS are known to be biosynthesized by a variety of bacteria only under phosphorus limitation, we  
854 suggest that they might serve as substitute lipids for the microorganisms in the OMZ. Since lipid  
855 substitutions have been observed in bacterial cultures at phosphate concentrations  $< 20 \mu\text{M}$ , conditions  
856 that are met in the OMZ of the ETNP and other oceanic systems that are generally not considered to be  
857 phosphorus limited, perhaps the paradigm of substitute lipids needs to be re-evaluated.

858

#### 859 **Author contribution**

860 SGW collected the samples. SGW, FS and KUH designed the study. SX and FS measured and processed  
861 the data. JSL and FS performed statistical analyses. FS, SX and SGW wrote the paper with input from  
862 KUH and JSL.

863

#### 864 **Competing interests**

865 The authors declare that they have no conflict of interest.

866



867 **Acknowledgments**

868 We are grateful to the captain and the crew of R/V *Seward Johnson*, to K. Daly and K. Wishner as co-  
869 chief scientists, and to the U.S. National Science Foundation for supporting the cruise. H. Albrecht, B.  
870 Olsen and S. Habtes helped with PM sampling. We thank K. Fanning and R. Masserini (University of  
871 South Florida) for providing their nutrient results; C. Flagg (Stony Brook) processed CTD hydrographic  
872 data; Jay Brandes and Mary Richards (Skidaway Institute) conducted the POC and TN analyses; B. Olson  
873 and K. Daly (University of South Florida) provided ship-board Chl-*a* analyses; and G. DeTullio (College  
874 of Charleston) conducted HPLC analyses of pigments. Lab supplies and analytical infrastructure for  
875 lipid analyses was funded by the Deutsche Forschungsgemeinschaft (DFG, Germany) through the Cluster  
876 of Excellence/Research Center MARUM. The UPLC-QTOF instrument was granted by the DFG,  
877 Germany through Grants Inst 144/300-1. S. Xie was funded by the China Scholarship Council, F. Schubotz  
878 by the Zentrale Forschungsförderung of the University of Bremen, and U.S. National Science Foundation  
879 grant OCE-0550654 to S. G. Wakeham supported this project. SGW also acknowledges a Fellowship from  
880 the Hanse-Wissenschaftskolleg (Hanse Institute for Advanced Studies) in Delmenhorst, Germany.

881

882 **References**

883 Andreou, A., Brodhun, F., Feussner, I.: Biosynthesis of oxylipins in non-mammals, *Progr. Lip. Res.*, 48,  
884 148-170, 2009.

885 Araki, S., Eichenberger, W., Sakurai, T., and Sato, N.: Distribution of  
886 diacylglycerylhydroxymethyltrimethyl- $\beta$ -alanine (DGTA) and phosphatidylcholine in brown algae,  
887 *Plant Cell Physiol.*, 32, 623-628, 1991.



- 888 Bale, N. J., Hopmans, E. C., Schoon, P. L., de Kluijver, A., Downing, J. A., Middelburg, J. J., Sinninghe  
889 Damsté, J. S. and Schouten, S.: Impact of trophic state on the distribution of intact polar lipids in  
890 surface waters of lakes. *Limnol. Oceanogr.*, 61, 1065–1077, 2016.
- 891 Basse, A., Zhu, C., Versteegh, G.J.M., Fischer, G., Hinrichs, K.-U., and Mollenhauer, G.: Distribution of  
892 intact and core tetraether lipids in water column profiles of suspended particulate matter off Cape  
893 Blank, NW Africa, *Org. Geochem.*, 72, 1-13, 2014.
- 894 Benning, C., Beatty, J. T., Prince, R. C., and Somerville C. R.: The sulfolipid  
895 sulfoquinovosyldiacylglycerol is not required for photosynthetic electron transport in *Rhodobacter*  
896 *sphaeroides* but enhances growth under phosphate limitation, *Proc. Natl. Acad. Sci. USA*, 90, 1561–  
897 1565, 1993.
- 898 Bianchi, M., Marty, D., Teyssié, J.-L., and Fowler, S. W.: Strictly aerobic and anaerobic bacteria  
899 associated with sinking particulate matter and zooplankton fecal pellets, *Mar. Ecol. Press Ser.*, 88, 55-  
900 60, 1992.
- 901 Bosak, T., Schubotz, F., de Santiago-Torio, A., Kuehl, J. V., Carlson, H. K., Watson, N., Daye, M.,  
902 Summons, R. E., Arkin, A. P., and Deutschbauer A. M.: System-Wide Adaptations of *Desulfovibrio*  
903 *alaskensis* G20 to Phosphate-Limited Conditions, *PLoS ONE* 11, e0168719, 2016.
- 904 Brandsma, J., Hopmans, E. C., Philippart, C. J. M., Veldhuis, M. J. W., Schouten, S., and Sinninghe  
905 Damste, J. S.: Low temporal variation in the intact polar lipid composition of North Sea coastal marine  
906 water reveals limited chemotaxonomic value, *Biogeosciences*, 9, 1073–1084, 2012.
- 907 Brett, M. T., and Müller-Navarra, D. C.: The role of highly unsaturated fatty acids in aquatic foodweb  
908 processes, *Freshw. Biol.*, 38, 483–499, 1997.



- 909 Carini P., Van Mooy B. A. S., Thrash J. C., White A., Zhao Y., Campbell E. O., Fredricks H. F., and  
910 Giovanni S. J.: SAR11 lipid renovation in response to phosphate starvation. *Proc. Natl. Acad. Sci.*  
911 USA, 112, 7767–7772, 2015.
- 912 Carolan, M.T., Smith, J.M., and Beman, J.M.: Transcriptomic evidence for microbial sulfur cycling in the  
913 eastern tropical North Pacific oxygen minimum zone. *Front. Microbiol.* 6, 334, 2015.
- 914 Cass, C. J., and Daly, K. L.: Ecological characteristics of eucalanoid copepods of the eastern tropical  
915 North Pacific Ocean: Adaptations for life within a low oxygen system, *J. Exp. Mar. Biol. Ecol.*, 468,  
916 118-129, 2015.
- 917 Cavan, E. L., Trimmer, M., Shelley, F., Sanders, R.: Remineralization of particulate organic carbon in an  
918 ocean oxygen minimum zone, *Nat. Comm.*, 8, 14847, 2016.
- 919 Codispoti, L. A., and Richards, F. A.: An analysis of the horizontal regime of denitrification in the eastern  
920 tropical North Pacific. *Limnology and Oceanography* 21, 379-388, 1976.
- 921 DeBaar, H. J. W., Farrington, J. W. and Wakeham, S. G.: Vertical flux of fatty acids in the North Atlantic  
922 Ocean, *J. Mar. Res.*, 41, 19-41, 1983.
- 923 DeLong, E. F. and Yayanos, A.: Biochemical function and ecological significance of novel bacterial lipids  
924 in deep-sea prokaryotes, *Appl. Environ. Microbiol.*, 51, 730-737, 1986.
- 925 Dembitsky, V.: Betaine ether-linked glycerolipids: Chemistry and biology, *Progr. Lip. Res.*, 35, 1-51,  
926 1996.
- 927 Diervo, A. J. and Reynolds, J. W.: Phospholipid composition and cardiolipin synthesis in fermentative  
928 and nonfermentative marine bacteria, *J. Bacteriol.* 123, 294-301, 1975.
- 929 DiTullio, G., and Geesey, M. E.: Photosynthetic Pigments in Marine Algae and Bacteria. In: G Bitton (ed),



- 930 Encyclopedia of Environmental Microbiology, vol. 5, Wiley, pp 2453-2470, 2002.
- 931 Elling, F. J., Könneke, M., Mußmann, M., Greve, A., and Hinrichs, K.-U.: Influence of temperature, pH,  
932 and salinity on membrane lipid composition and TEX86 of marine planktonic thaumarchaeal isolates,  
933 *Geochim. Cosmochim. Acta*, 171, 238-255, 2015.
- 934 Elling, F. J., Könneke, M., Nicol, G. W., Stieglmeier, M., Bayer, B., Spieck, E., La Torre, De J. R., Becker,  
935 K. W., Thomm, M., Prosser, J. I., Herndl, G. J., Schleper, C., and Hinrichs, K.-U. Chemotaxonomic  
936 characterisation of the thaumarchaeal lipidome, *Environ. Microbiol.* 10, 1080, 2017.
- 937 Ertefai, T., Fisher, M., Fredricks, H. and Lipp, J.: Vertical distribution of microbial lipids and functional  
938 genes in chemically distinct layers of a highly polluted meromictic lake, *Org. Geochem.*, 39, 1572-  
939 1588, 2008.
- 940 Exterkate, F. A., and Veerkamp, J. H.: Biochemical changes in *Bifidobacterium bifidum* var.  
941 *Pennsylvanicus* after cell wall inhibition. I. Composition of lipids, *Biochim. Biophys. Acta*, 176, 65-  
942 77, 1969.
- 943 Fiedler, P. C., and Talley, L. D.: Hydrography of the eastern tropical Pacific: A review. *Progr. Oceanogr.*,  
944 69, 143-180, 2006.
- 945 Franck, V. M., Smith, G. J., Bruland, K. W., and Brzezinski, M. A.: Comparison of size-dependent carbon,  
946 nitrate and silicic acid uptake rates in high- and low-iron waters. *Limnol. Oceanogr.*, 50, 825-838,  
947 2005.
- 948 Geiger, O., González-Silva, N., López-Lara, I. M., and Sohlenkamp, C.: Amino acid-containing  
949 membrane lipids in bacteria, *Progr. Lip. Res.*, 49, 46-60, 2010.
- 950 Geiger, O., Röhrs, V., Weissenmayer, B., Finan, T. M., and Thomas-Oates, J. E.: The regulator gene *phoB*



- 951 mediates phosphate stress-controlled synthesis of the membrane lipid diacylglyceryl-N,N,N-
- 952 trimethylhomoserine in *Rhizobium* (*Sinorhizobium*) *meliloti*, *Mol. Microbiol.*, 32, 63–73, 1999.
- 953 Geske, T., Dorp vom, K., Dörmann, P., and Hölzl G.: Accumulation of glycolipids and other non-
- 954 phosphorous lipids in *Agrobacterium tumefaciens* grown under phosphate deprivation, *Glycobiol.*, 23,
- 955 69–80, 2012.
- 956 Goericke, R., Olson, R. J., and Shalapyonok, A.: A novel niche for *Prochlorococcus* sp. in low-light
- 957 suboxic environments in the Arabian Sea and the Eastern Tropical North Pacific, *Deep Sea Res. I*, 47,
- 958 1183-1205, 2000.
- 959 Goldfine, H.: Bacterial membranes and lipid packing theory, *J. Lip. Res.*, 25, 1501–1507, 1984.
- 960 Goldfine, H., and Ellis, M. E.: N-methyl groups in bacterial lipids, *J. Bacteriol.*, 87, 8–15, 1964.
- 961 Gruber, N.: The marine nitrogen cycle: overview and challenges, in: *Nitrogen in the marine environment*,
- 962 Eds. DG Capone, DA Bronk, MR Mulholland, EJ Carpenter, Burlington, MA, USA: Academic, 1-50,
- 963 2008.
- 964 Harvey, R. H., Fallon R. D., and Patton, J. S.: The effect of organic matter and oxygen on the degradation
- 965 of bacterial membrane lipids in marine sediments, *Geochim. Cosmochim. Acta*, 50, 795-804, 1986.
- 966 Hernandez-Sanchez, M. T., Homoky, W. B., and Pancost, R. D.: Occurrence of 1-O-monoalkyl glycerol
- 967 ether lipids in ocean waters and sediment, *Org. Geochem.* 66, 1–13, 2014.
- 968 Hölzl, G., and Dörmann, P.: Structure and function of glycolipids in plants and bacteria, *Progr.*
- 969 *Lip. Res.* 46, 225–243, 2007.
- 970 Hurley, S. J., Elling, F. J., Könneke, M., Buchwald, C., Wankel, S. D., Santoro, A. E., Lipp, J. S., Hinrichs,
- 971 K.-U., and Pearson, A.: Influence of ammonia oxidation rate on thaumarchaeal lipid composition and



- 972 the TEX86 temperature proxy, *Proc. Natl. Acad. Sci. USA*, 113, 7762-7767, 2016.
- 973 Kalvelage, T., Lavik, G., Jensen, M. M., Revsbech, N. P., Löscher, C., Schunck, H., Desai, D. K., Hauss,  
974 H., Kiko, R., Holtappels, M., LaRoche, J., Schmitz, R. A., Graco, M. I., and Kuypers, M. M. M.:  
975 Aerobic microbial respiration in oceanic oxygen minimum zones, *PLoS ONE*, 10(7):e0133526, 2015.
- 976 Karstensen, J., Stramma L., and Visbeck M.: Oxygen minimum zones in the eastern tropical Atlantic and  
977 Pacific oceans, *Progr. Oceanogr.*, 77, 331-350, 2008.
- 978 Kato, T., Yamaguchi, Y., Hirano, T., and Yokoyama, T.: Unsaturated hydroxy fatty acids, the self  
979 defensive substances in rice plant against rice blast disease, *Chem. Let.*, 409-412, 1984.
- 980 Keeling, R. F., Körtzinger, A., and Gruber N.: Ocean deoxygenation in a warming world, *Annu. Rev.*  
981 *Marine. Sci.*, 2, 199–229, 2010.
- 982 Lam, P. and Kuypers, M. M. M.: Microbial nitrogen cycling processes in oxygen minimum zones, *Annu.*  
983 *Rev. Marine. Sci.*, 3, 317–345, 2011.
- 984 Landry, M. R., Selph, K. E., Taylor, A.G., Décima, M., Balch, W. M., and Bidigare R. R.: Phytoplankton  
985 growth, grazing and production balances in the HNLC equatorial Pacific, *Deep Sea Res. I*, 58, 524-  
986 535, 2011.
- 987 Lavín, M. F., Fiedler, P. C., Amador, J. A., Balance, L. T., Färber-Lorda, J., Mestas-Nuñez, A. M.: A  
988 review of eastern tropical Pacific oceanography: Summary, *Progr. Oceanogr.*, 69, 391-398, 2006.
- 989 Lee C., and Cronin C.: Particulate amino acids in the sea: Effects of primary productivity and biological  
990 decomposition, *J. Mar. Res.*, 42, 1075-1097, 1984.
- 991 Lehninger A. L.: Oxidation of fatty acids, in: *Biochemistry*, New York: Worth, 417-432, 1970.
- 992 Lin, X., Wakeham, S. G., Putnam, I. F., Astor, Y. M., Scranton, M. I., Chistoserdov, A. Y., and Taylor, G.





- 993 T.: Comparison of vertical distributions of prokaryotic assemblages in the anoxic Cariaco Basin and  
994 Black Sea by use of fluorescence in situ hybridization, *Appl. Environ. Microbiol.*, 72, 2679-2690,  
995 2006.
- 996 Lincoln, S. A., Wai, B., Eppley, J. M., Church, M. J., Summons, R. E. and DeLong, E. F.: Planktonic  
997 Euryarchaeota are a significant source of archaeal tetraether lipids in the ocean, *Proc. Natl. Acad. Sci.*  
998 USA, 111, 9858–9863, 2014.
- 999 Logemann, J., Graue, J., Köster, J., Engelen, B., Rullkötter, J., and Cypionka, H.: A laboratory experiment  
1000 of intact polar lipid degradation in sandy sediments, *Biogeosci.*, 8, 2547-2560, 2011.
- 1001 Lynch, D. V., and Dunn, T. M.: An introduction to plant sphingolipids and a review of recent advances in  
1002 understanding their metabolism and function, *New Phytol.*, 161, 677-702, 2004.
- 1003 Ma, Y., Zeng, Y., Jiao, N., Shi, Y., and Hong, N.: Vertical distribution and phylogenetic composition of  
1004 bacteria in the Eastern Tropical North Pacific Ocean, *Microbiol. Res.*, 164, 624-663, 2009.
- 1005 Maas, A. E., Frazar, S. L., Outram, D.M., Seibel, B. A., and Wishner, K. F.: Fine-scale vertical  
1006 distributions of macroplankton and micronekton in the Eastern Tropical North Pacific in association  
1007 with an oxygen minimum zone, *J Plankt. Res.*, 36, 1557-1575, 2014.
- 1008 Mackender, R. O., and Leech, R. M.: The galactolipid, phospholipid, and fatty acid composition of the  
1009 chloroplast envelope membranes of *Vicia Faba* L, *Plant Physiol.*, 53, 496-502, 1974.
- 1010 Matos, A. R., and Pham-Thi, A.-T.: Lipid deacylating enzymes in plants: Old activities, new genes. *Plant*  
1011 *Physiology and Biochemistry* 47, 491-503, 2009.
- 1012 Meador, T. B., Gagen, E. J., Loscar, M. E., Goldhammer, T., Yoshinaga, M. Y., Wendt, J., Thomm, M.,  
1013 and Hinrichs, K.-U.: *Thermococcus kodakarensis* modulates its polar membrane lipids and elemental



- 1014 composition according to growth state and phosphate availability, *Front. Microbiol.*, 5:10,  
1015 doi:10.3389/fmicb.2014.00010, 2014.
- 1016 Mileykovskaya, E., and Dowhan, W.: Cardiolipin membrane domains in prokaryotes and eukaryotes,  
1017 *Biochim. Biophys. Acta* 1788, 2084–2091, 2009.
- 1018 Morita, Y. S., Yamaryo-Botte, Y., and Miyanagi, K.: Stress-induced synthesis of phosphatidylinositol 3-  
1019 phosphate in mycobacteria, *J. Biol. Chem.* 285, 16643-16650, 2010.
- 1020 Neal, A. C., Prahl, F. G., Eglinton, G., O'Hara, S. C. M., and Corner, E. D. S.: Lipid changes during a  
1021 planktonic feeding sequence involving unicellular algae, Elminius Nauplii and Adult Calanus, *J. Mar.*  
1022 *Biol. Assoc. UK*, 66, 1-13, 1986.
- 1023 Nishihara, M., Yokota, K., and Kito, M.: Lipid molecular species composition of thylakoid membranes,  
1024 *Biochim. Biophys. Acta*, 617, 12-19, 1980.
- 1025 Oliver, J. D., and Colwell, R. R.: Extractable lipids of gram-negative marine bacteria: Phospholipid  
1026 composition, *J. Bacteriol.* 114, 897-908, 1973.
- 1027 Olson, M. B., and Daly, K. L.: Micro-grazer biomass, composition and distribution across prey resource  
1028 and dissolved oxygen gradients in the far eastern tropical north Pacific Ocean, *Deep Sea Res. I*, 75,  
1029 28-38, 2014.
- 1030 Okuyama, H., Kogame, K., and Takeda, S.: Phylogenetic significance of the limited distribution of  
1031 octadecapentaenoic acid in prymnesiophytes and photosynthetic dinoflagellates, *Proc. NIPR Symp.*  
1032 *Polar Biol.*, 6, 21–26, 1993.
- 1033 Parsons, T. R., Takahashi, M., and Hargrave B. (Eds.): *Biological Oceanographic Processes*, 3<sup>rd</sup> ed.,  
1034 Pergamon Press, NY, 1984.



- 1035 Paulmier, A., and Ruiz-Pino, D.: Oxygen minimum zones (OMZs) in the modern ocean, *Progr. Oceanogr.*  
1036 80, 113-128, 2009.
- 1037 Pennington, J. T., Mahoney, K. L., Kuwahara, V. S., Kolber, D. D., Cienes, R., Chavez, F. P.: Primary  
1038 production in the eastern tropical Pacific: A review, *Progr. Oceanogr.*, 69, 285-317, 2006.
- 1039 Pitcher, A., Villanueva, L., Hopmans, E. C., Schouten, S., Reichart, G.-J. and Sinninghe Damsté, J. S.:  
1040 Niche segregation of ammonia-oxidizing archaea and anammox bacteria in the Arabian Sea oxygen  
1041 minimum zone, *ISME J.*, 5, 1896–1904, 2011.
- 1042 Podlaska, A., Wakeham, S. G., Fanning, K. A., and Taylor, G. T.: Microbial community structure and  
1043 productivity in the oxygen minimum zone of the eastern tropical North Pacific, *Deep-Sea Res. Part I*,  
1044 66, 77–89, 2012.
- 1045 Poincelot, R.P.: Isolation and lipid composition of spinach chloroplast envelope membranes, *Arch.*  
1046 *Biochem. Biophys.*, 159, 134-142, 1973.
- 1047 Pependorf, K., Lomas, M., and Van Mooy, B.: Microbial sources of intact polar diacylglycerolipids in the  
1048 Western North Atlantic Ocean, *Org. Geochem.* 42, 803-811, 2011a.
- 1049 Pependorf, K. J., Tanaka, T., Pujo-Pay, M., Lagaria, A., Courties, C., Conan, P., Oriol, L., Sofen, L. E.,  
1050 Moutin, T., and Van Mooy, B. A. S.: Gradients in intact polar diacylglycerolipids across the  
1051 Mediterranean Sea are related to phosphate availability, *Biogeosci.* 8, 3733–3745, 2011b.
- 1052 Prahl, F. G., Eglinton, G., Corner, E. D. S., O'Hara, D. C. M., and Forsberg, T. E. V.: Changes in plant  
1053 lipids during passage through the gut of *Calanus*, *J. Mar. Biol. Assoc. UK*, 1984.
- 1054 Rabinowitz, G. B.: An introduction to nonmetric multidimensional scaling, *Amer. J. Polit. Sci.*, 343-90,  
1055 1975.



- 1056 Rappé, M. S., and Giovannoni, S. J.: The uncultured microbial majority, *Annu. Rev. Microbiol.*, 57, 369-  
1057 394, 2003.
- 1058 Richards, F. A.: Anoxic basins and fjords, in: Ripley JP, Skirrow G (Eds.) *Chemical Oceanography*.  
1059 Academic Press, London and New York, 611-645, 1965.
- 1060 Rojas-Jiménez, K., Sohlenkamp, C., Geiger, O., Martínez-Romero, E., Werner, D., and Vinuesa, P.: A  
1061 CIC chloride channel homolog and ornithine-containing membrane lipids of rhizobium tropici  
1062 CIAT899 are involved in symbiotic efficiency and acid tolerance, *Mol. Plant-Microbe Interact.*, 18,  
1063 1175–1185, 2005.
- 1064 Rush, D., Wakeham, S. G., Hopmans, E. C., Schouten, S., and Damsté, J. S. S.: Biomarker evidence for  
1065 anammox in the oxygen minimum zone of the Eastern Tropical North Pacific, *Org. Geochem.*, 53,  
1066 80–87, 2012.
- 1067 Rütters, H., Sass, H., Cypionka, H., and Rullkötter, J.: Monoalkylether phospholipids in the sulfate-  
1068 reducing bacteria *Desulfosarcina variabilis* and *Desulforhabdus amnigenus*, *Arch. Microbiol.*, 176,  
1069 435–442, 2011.
- 1070 Schouten, S., Pitcher, A., Hopmans, E. C., Villanueva, L., Van Bleijswijk, J., and Sinninghe Damsté, J.  
1071 S.: Intact polar and core glycerol dibiphytanyl glycerol tetraether lipids in the Arabian Sea oxygen  
1072 minimum zone: I. Selective preservation and degradation in the water column and consequences for  
1073 the TEX86, *Geochim. Cosmochim. Acta*, 98, 228–243, 2012.
- 1074 Schubotz, F., Wakeham, S. G., Lipp, J., Fredricks, H. F., and Hinrichs, K.-U.: Detection of microbial  
1075 biomass by intact polar membrane lipid analysis in the water column and surface sediments of the  
1076 Black Sea, *Environ. Microbiol.*, 11, 2720-2734, 2009.



- 1077 Sebastian, M., Smith, A. F., González, J. M., Fredricks, H. F., Van Mooy, B., Koblížek, M., Brandsma,  
1078 J., Koster, G., Mestre, M., Mostajir, B., Pitta, P., Postle, A. D., Sánchez, P., Gasol, J. M., Scanlan, D.  
1079 J., and Chen, Y.: Lipid remodelling is a widespread strategy in marine heterotrophic bacteria upon  
1080 phosphorus deficiency, *ISME J*, 10, 968–978, 2016.
- 1081 Seibel, B.A.: Critical oxygen levels and metabolic suppression in oceanic oxygen minimum zones, *J. Exp.*  
1082 *Biol.*, 214, 326-336, 2011.
- 1083 Seidel, M., Graue, J., Engelen, B., Köster, J., Sass, H., and Rullkötter, J.: Advection and diffusion  
1084 determine vertical distribution of microbial communities in intertidal sediments as revealed by  
1085 combined biogeochemical and molecular biological analysis, *Org. Geochem.*, 52, 114–129, 2012.
- 1086 Shanks, A. L., and Reeder, M. L.: Reducing microzones and sulfide production in marine snow. *Marine*  
1087 *Ecology Press Series* 96, 43-47, 1993.
- 1088 Sherr, E. B., and Sherr B. F.: Significance of predation by protists in aquatic microbial food webs, *Antonie*  
1089 *van Leeuwenhoek* 81, 293-308, 2002.
- 1090 Siegenthaler P.-A.: Molecular organization of acyl lipids in photosynthetic membranes of higher plants,  
1091 in: *Lipids in Photosynthesis*, Siegenthaler, P.-A., and Murata, N. (Eds). Dordrecht, the Netherlands:  
1092 Kluwer Academic Publishers, 119–144, 1998.
- 1093 Sohlenkamp, C., López-Lara, I. M., and Geiger, O.: Biosynthesis of phosphatidylcholine in bacteria, *Progr.*  
1094 *Lip. Res.*, 42, 115–162, 2003.
- 1095 Sollai, M., Hopmans, E. C., Schouten, S., Keil, R. G., and Sinninghe Damsté, J.S.: Intact polar lipids of  
1096 Thaumarchaeota and anammox bacteria as indicators of N cycling in the eastern tropical North Pacific  
1097 oxygen-deficient zone, *Biogeosci.*, 12, 4833-4864, 2015.



- 1098 Stevens H., and Ulloa, O.: Bacterial diversity in the oxygen minimum zone of the eastern tropical South  
1099 Pacific, *Environ. Microbiol.*, 10, 1244–1259, 2008.
- 1100 Stramma, L., Johnson, G. C., Sprintall, J., and Mohrholz, V.: Expanding Oxygen-Minimum Zones in the  
1101 Tropical Oceans, *Science*, 320, 655-658, 2008.
- 1102 Stramma, L., Schmidtko, S., Levin, L. A., and Johnson, G. C.: Ocean oxygen minima expansions and their  
1103 biological impacts, *Deep Sea Res. I*, 57, 587-595, 2010.
- 1104 Sturt, H. F., Summons, R. E., Smith, K.E., Elvert, M., Hinrichs, K.-U.: Intact polar membrane lipids in  
1105 prokaryotes and sediments deciphered by high-performance liquid chromatography/electrospray  
1106 ionization multistage mass spectrometry - new biomarkers for biogeochemistry and microbial ecology,  
1107 *Rapid Comm. Mass Spec.*, 18, 617-628, 2004.
- 1108 Taylor, G. T., Iabichella, M., Ho, T.-Y., Scranton, M. I., Thunell, R. C., Muller-Karger, F., and Varela R.:  
1109 Chemoautotrophy in the redox transition zone of the Cariaco Basin: A significant midwater source of  
1110 organic carbon production, *Limnol. Oceanogr.*, 46, 148-163, 2001.
- 1111 Thompson, G. A.: Lipids and membrane function in green algae, *Biochim. Biophys. Acta*, 1302, 17-45,  
1112 1996.
- 1113 Tiano, L., Garcia-Robledo, E., Dalsgaard, T., Devol, A. H., Ward, B. B., Ulloa, O., Canfield, D. E., and  
1114 Revsbech, N. P.: Oxygen distribution and aerobic respiration in the north and south eastern tropical  
1115 Pacific oxygen minimum zones, *Deep Sea Res. I*, 94, 173-183, 2014.
- 1116 Turich, C., and Freeman, K. H.: Archaeal lipids record paleosalinity in hypersaline systems, *Org.*  
1117 *Geochem.* 42, 1147-1157, 2011.
- 1118 Ulloa, O., Canfield, D., DeLong, E. F., Letelier, R. M., and Stewart, F. J.: Microbial oceanography of



- 1119 anoxic oxygen minimum zones, *Proc. Natl. Acad. Sci., USA* 109, 15996-16003, 2012.
- 1120 Valentine, R. C., and Valentine, D. L.: Omega-3 fatty acids in cellular membranes: a unified concept,  
1121 *Progr. Lip. Res.* 43, 383–402, 2004.
- 1122 Van Mooy, B. A. S., and Fredricks, H. F.: Bacterial and eukaryotic intact polar lipids in the eastern  
1123 subtropical South Pacific: Water-column distribution, planktonic sources, and fatty acid composition,  
1124 *Geochim. Cosmochim. Acta*, 74, 6499–6516, 2010.
- 1125 Van Mooy, B. A. S., Fredricks, H. F., Pedler, B. E., Dyhrman, S. T., Karl, D. M., Koblížek, M., Lomas,  
1126 M. W., Mincer, T. J., Moore, L. R., Moutin, T., Rappé, M. S., and Webb, E. A.: Phytoplankton in the  
1127 ocean use non-phosphorus lipids in response to phosphorus scarcity, *Nature*, 458, 69–72, 2009.
- 1128 Van Mooy, B. A. S., Rocap, G., Fredricks, H. F., Evans, C. T., and Devol, A. H.: Sulfolipids dramatically  
1129 decrease phosphorus demand by picocyanobacteria in oligotrophic marine environments, *Proc. Natl.*  
1130 *Acad. Sci. USA*, 103, 8607–8612, 2006.
- 1131 Vardi, A., Van Mooy, B. A. S., Fredricks, H. F., Popen Dorf, K. J., Ossolinski, J. E., Haramty, L., and Bidle,  
1132 K. D.: Viral glycosphingolipids induce lytic infection and cell death in marine phytoplankton, *Science*,  
1133 326, 861-865, 2009.
- 1134 Wada, H., and Murata, N.: Membrane Lipids in cyano- bacteria, in: *Lipids in Photosynthesis: Structure,*  
1135 *Function and Genetics*, Siegenthaler, P., and Murata, N. (Eds), Dordrecht, the Netherlands: Kluwer  
1136 Academic Publishers, 65–81, 1998.
- 1137 Wakeham, S. G., Turich, C., Schubotz, F., Podlaska, A., Li, X. N., Varela, R., Astor, Y., Sáenz, J. P.,  
1138 Rush, D., Sinninghe Damsté, J. S., Summons, R. E., Scranton, M. I., Taylor, G. T., and Hinrichs, K.-  
1139 U.: Biomarkers, chemistry and microbiology show chemoautotrophy in a multilayer chemocline in



- 1140 the Cariaco Basin, *Deep Sea Res. Part I*, 63, 133–156, 2012.
- 1141 Wakeham, S. G., Amann, R., Freeman, K. H., Hopmans, E. C., Jørgensen, B. B., Putnam, I. F., Schouten,  
1142 S., Sinninghe Damsté, J. S., Talbot, H. M., and Woebken, D.: Microbial ecology of the stratified water  
1143 column of the Black Sea as revealed by a comprehensive biomarker study, *Org. Geochem.*, 38, 2070–  
1144 2097, 2007.
- 1145 Wakeham, S. G.: Monocarboxylic, dicarboxylic and hydroxy acids released by sequential treatments of  
1146 suspended particles and sediments of the Black Sea, *Org. Geochem.* 30, 1059-1074, 1999.
- 1147 Wakeham, S. G.: Reduction of stenols to stanols in particulate matter at oxic-anoxic boundaries in sea  
1148 water, *Nature*, 342, 787-790, 1989.
- 1149 Wakeham, S. G., and Canuel, E. A.: Organic geochemistry of particulate matter in the eastern tropical  
1150 North Pacific Ocean: Implications for particle dynamics, *J. Mar. Res.*, 46, 182-213, 1988.
- 1151 Wakeham, S. G.: Steroid geochemistry in the oxygen minimum zone of the eastern tropical North Pacific  
1152 Ocean, *Geochim. Cosmochim. Acta*, 51, 3051-3069, 1987.
- 1153 Williams, R. L., Wakeham, S., McKinney, R., Wishner, K. F.: Trophic ecology and vertical patterns of  
1154 carbon and nitrogen stable isotopes in zooplankton from oxygen minimum zone regions, *Deep Sea*  
1155 *Res. I*, 90 36-47, 2014.
- 1156 Wishner, K. F., Outram, D. M., Seibel, B. A., Daly, K. L., and Williams, R. L.: Zooplankton in the eastern  
1157 tropical north Pacific: Boundary effects of oxygen minimum zone expansion, *Deep Sea Res. I*, 79,  
1158 122-140, 2013.
- 1159 Wishner, K. F., Gelfman, C., Gowing, M. M., Outram, D. M., Rapien, M., and Williams, R. L.: Vertical  
1160 zonation and distributions of calanoid copepods through the lower oxycline of the Arabian Sea oxygen





- 1161 minimum zone, *Progr. Oceanogr.*, 78, 163-191, 2008.
- 1162 Wuebken, D., Fuchs, B. M., Kuypers, M. M. M, and Aman, R.: Potential interactions of particle-associated  
1163 anammox bacteria with bacterial and archaeal partners in the Namibian upwelling system, *Appl.*  
1164 *Environ. Microbiol.*, 73, 4648-4657, 2007.
- 1165 Wörmer, L., Lipp, J. S., Schröder, J. M., and Hinrichs, K.-U.: Application of two new LC-ESI-MS  
1166 methods for improved detection of intact polar lipids (IPLs) in environmental samples, *Org. Geochem.*  
1167 59, 10–21, 2013.
- 1168 Wright, J. J., Konwar, K. M., and Hallam, S. J: Microbial ecology of expanding oxygen minimum zones,  
1169 *Nat. Rev. Microbiol.* 10, 381-394, 2012.
- 1170 Xie, S., Liu, X.-L., Schubotz, F., Wakeham, S. G., and Hinrichs K.-U.: Distribution of glycerol ether lipids  
1171 in the oxygen minimum zone of the Easter Tropical North Pacific Ocean, *Org. Geochem.* 71, 60–71,  
1172 2014.
- 1173 Yao, M., Elling, F. J., Jones, C., Nomosatryo, S., Long, C. P., Crowe, S. A., Antoniewicz, M. R., Hinrichs,  
1174 K.-U., and Maresca, J. A.: Heterotrophic bacteria from an extremely phosphate-poor lake have  
1175 conditionally reduced phosphorus demand and utilize diverse sources of phosphorus, *Environ.*  
1176 *Microbiol.* 18, 656–667, 2015.
- 1177 Zavaleta-Pastor, M., Sohlenkamp, C., Gao, J. L., Guan, Z., Zaheer, R., Finan, T. M., Raetz, C. R. H.,  
1178 López-Lara, I. M., and Geiger, O.: *Sinorhizobium meliloti* phospholipase C required for lipid  
1179 remodeling during phosphorus limitation, *Proc. Natl. Acad. Sci. USA*, 107, 302–307, 2010.
- 1180 Zhang, Y.-M., and Rock, C. O.: Membrane lipid homeostasis in bacteria, *Nat. Rev. Microbiol.*, 6, 222–  
1181 233, 2008.



1182 Zhu, C., Wakeham, S. G., Elling, F. J., Basse, A., Mollenhauer, G., Versteegh, G. J. M., Könneke, M.,  
1183 and Hinrichs, K.-U.: Stratification of archaeal membrane lipids in the ocean and implications for  
1184 adaptation and chemotaxonomy of planktonic archaea, *Environ. Microbiol.* 18, 4324-4336, 2016.  
1185



1186 **Tables**

1187 **Table 1.** Spearman Rank Order Correlation coefficients (r) for data combined from all four stations. Only  
 1188 significant correlations, where 0.05 (highly significant  $p < 0.001$ , in bold), are presented.

	Glycolipids				Aminolipids				Phospholipids							
	% GL	% 1G	% 2G	% SQ	% GL:PL	% SQ:PG	% AL	% DGTS	% AL:PL	% DGTS:PC	% PL	% PC	% PG	% PE	% PME	% PDME
Depth	-	-	-	-	-0.41	<b>-0.76</b>										
Fluorescence	0.32				<b>0.67</b>											
POC					<b>0.63</b>	<b>0.67</b>										
TN					<b>0.61</b>	<b>0.6</b>										
Oxygen	<b>0.57</b>	0.3	<b>0.48</b>	0.35	<b>0.55</b>	<b>0.58</b>		0.36			-	-	-	-	-0.46	-0.52
Temperature	0.3				<b>0.52</b>	<b>0.63</b>	0.39	<b>0.69</b>			<b>0.49</b>		0.38	0.33		
Chl a	0.35				<b>0.72</b>	<b>0.71</b>	0.42	0.78								-0.33
Phosphate					-	-	-0.4	<b>-0.56</b>								0.36
Nitrate																
Nitrite																0.3
Ammonium		0.33							0.41	0.42	0.35	0.4				
N:P					-0.3	-										
						0.32										0.36

Abbreviations: GL – glycolipids, 1G – monoglycosyl, 2G – diglycosyl, SQ – sulfoquinovosyl, PL – phospholipids, AL – aminolipids, DGTS – diacylglycerol trimethyl homoserine, PC – phosphatidyl choline, PG – phosphatidyl glycerol, PE – phosphatidyl ethanolamine, PME – phosphatidyl methyl-ethanolamine, PDME – phosphatidyl dimethyl-ethanolamine

1189



1190 **Figures**

1191 **Figure 1.** a) Map of ETNP with R/V *Seward Johnson* (November 2007) cruise sampling stations. Depth  
1192 profiles of (b) oxygen, (c) temperature, (d) chlorophyll- $\alpha$  and (e) transmissivity along a northwest-  
1193 southeast transect of the study area. Numbers across the top panels denote station, black dots are  
1194 individual samples.

1195

1196 **Figure 2.** Section plots of major macronutrients along a northwest-southeast transect of the ENTP up to  
1197 1300 m water depth: (a) nitrate, (b) nitrite, (c) ammonium, (d) phosphate, (e) N:P (dissolved) is the sum  
1198 of total dissolved nitrogen species (nitrate, nitrite and ammonium) over phosphate, and (f) C:N (SPM) is  
1199 total carbon over total nitrogen of the solid phase collected by water filtration. Note that C:N is only  
1200 analyzed for  $<53 \mu\text{m}$  particle fraction. Numbers across the top panels denote station, black dots are  
1201 individual samples.

1202

1203 **Figure 3.** Absolute abundance of (a) particulate organic matter (POC) and (b) intact polar lipids (IPL) as  
1204 well as (c) the ratio of their concentration are shown for stations 1, 2, 5 and 8. Note that POC and IPL/POC  
1205 are only analyzed for the  $<53 \mu\text{m}$  particle fraction. Also shown are (d) absolute cell abundance and  
1206 relative proportions of (e) archaeal cells and (d) unclassified cells at the same stations. Numbers across  
1207 the top panels denote station, black dots are individual samples.

1208

1209 **Figure 4.** Relative abundance of (a) major and (b) minor IPLs at sampled depths of stations 1, 2, 5, and 8  
1210 in the ETNP. Major IPLs are defined as those comprising more than 10% of total IPLs (minor compounds



1211 comprised less than 10%) at more than one depth horizon at the four stations. Also depicted are the  
1212 different geochemical zones in the water column.

1213

1214 **Figure 5.** Relative abundance of IPLs along a northwest-southeast transect from station 1 to 8 grouped by  
1215 headgroup: total non-archaeal (a) phospholipids, (b) aminolipids, and (c) glycolipids are shown as percent  
1216 of total IPLs. The ratios of non-phospholipids to phospholipids are shown for (a) SQ-DAG to PG-DAG,  
1217 (e) DGTS to PC-DAG, and (f) 1G-DAG to PE-DAG. Numbers across the top panels denote station, black  
1218 dots are individual samples.

1219

1220 **Figure 6.** Changes in average chain length (CL) and number of double bonds (DB) of major IPLs detected  
1221 at stations 1, 2, 5 and 8 in the ETNP.

1222

1223 **Figure 7.** Nonmetric multidimensional scaling (NMDS) ordination plot assessing the relationship between  
1224 IPL biomarkers, sampling depths and geochemical parameters in the ETNP (stress=0.125). Squares  
1225 represent the water depth of each sample and are color-coded according to the defined geochemical  
1226 zonation. Filled circles stand for lipid distribution of major IPLs and open circles for minor IPLs on the  
1227 ordination. Vector lines of geochemical parameters are weighted by their p-values with each NMDS axis.  
1228



fig01

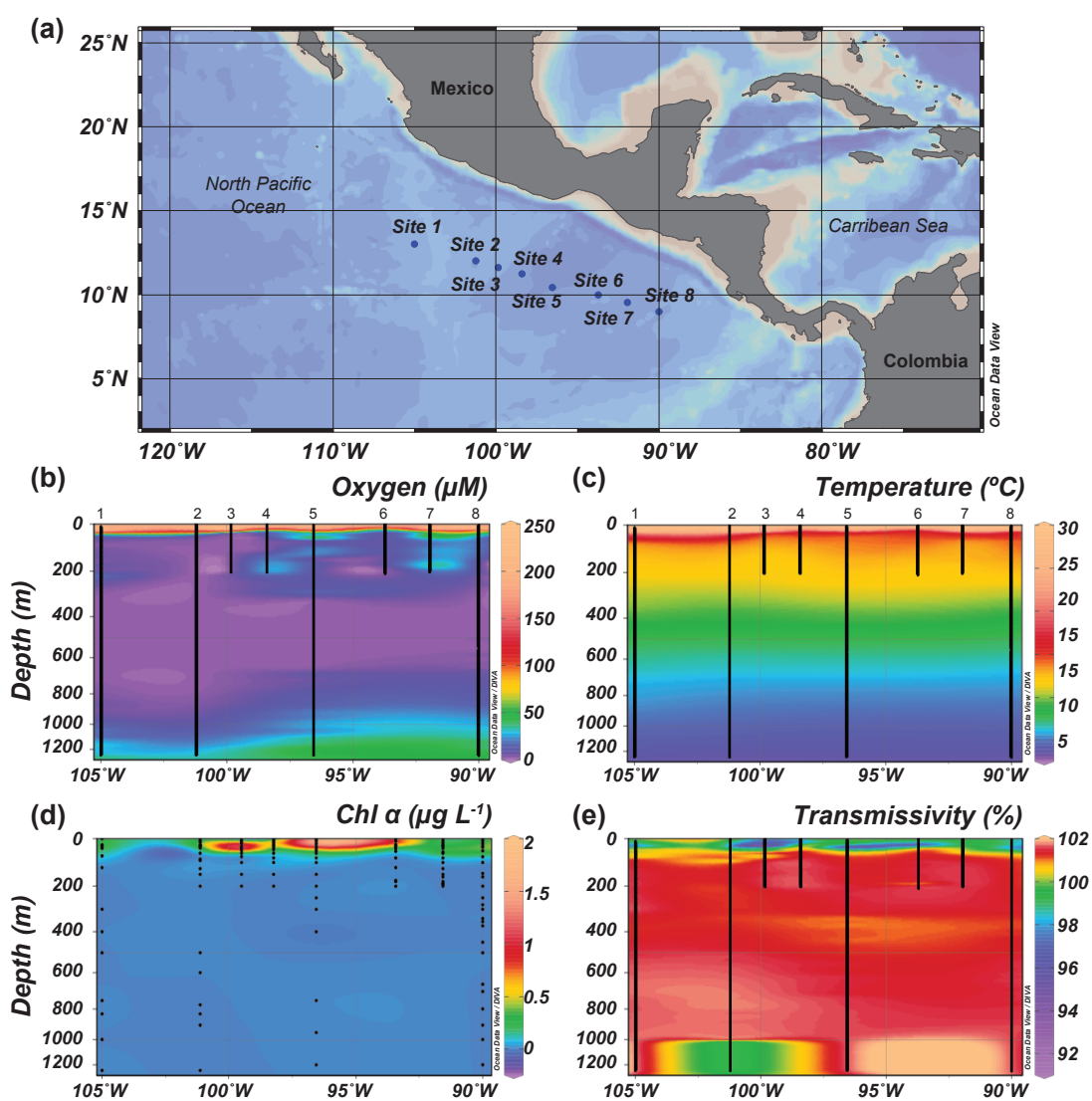




fig02

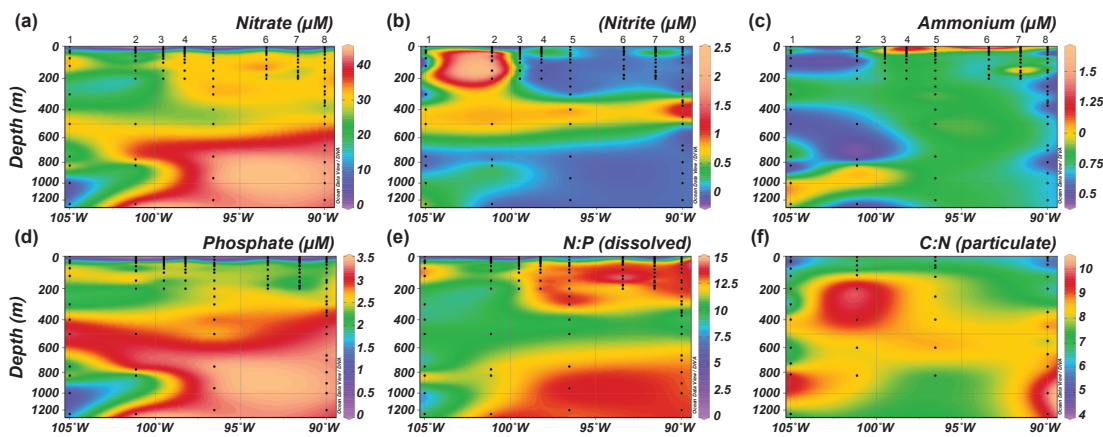




fig03

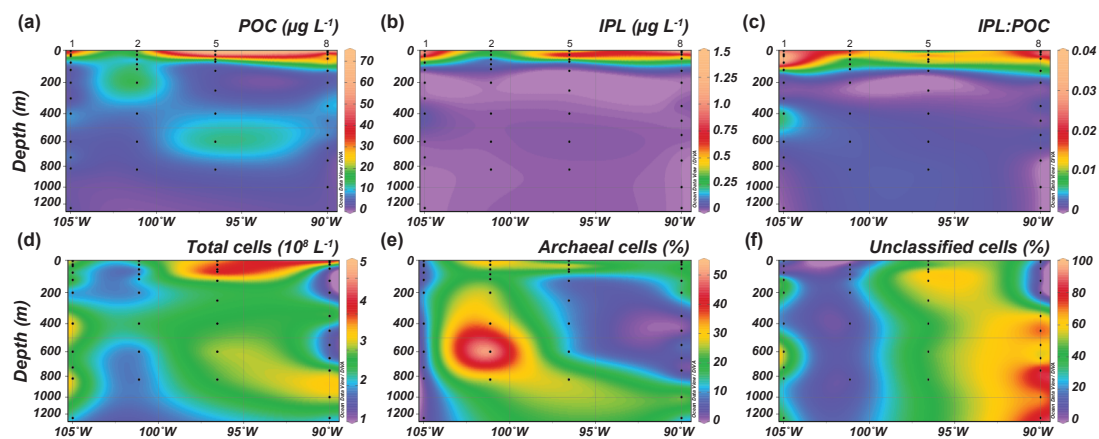






fig04

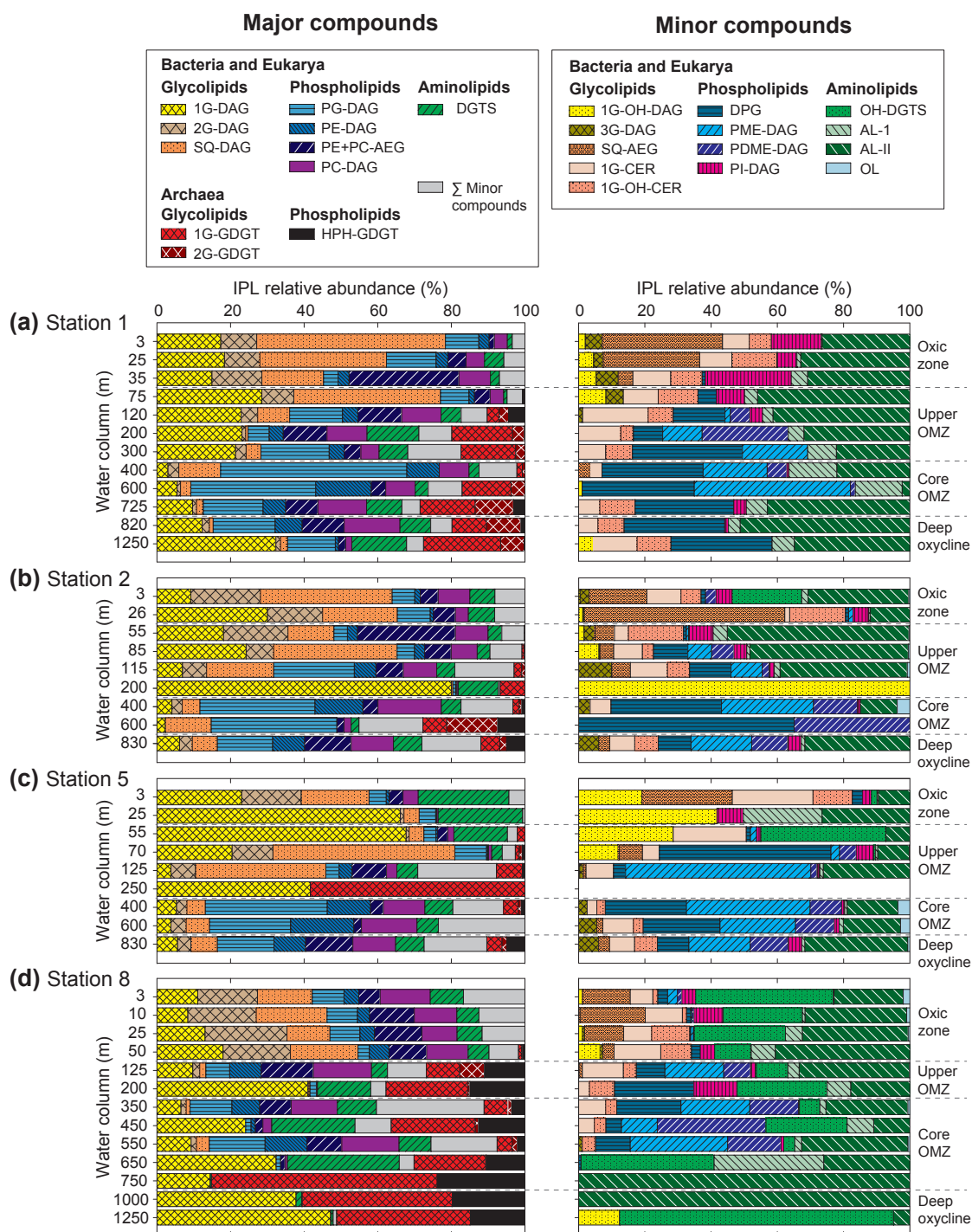




fig05

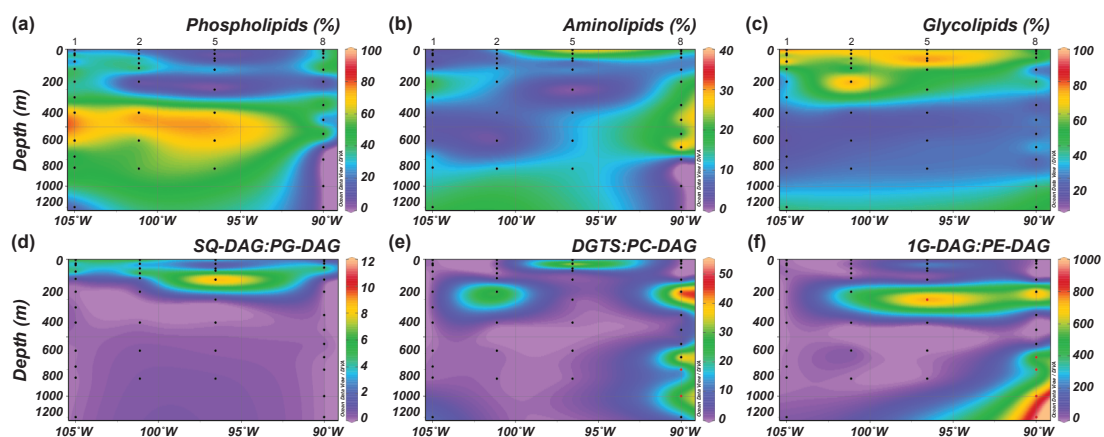




fig06

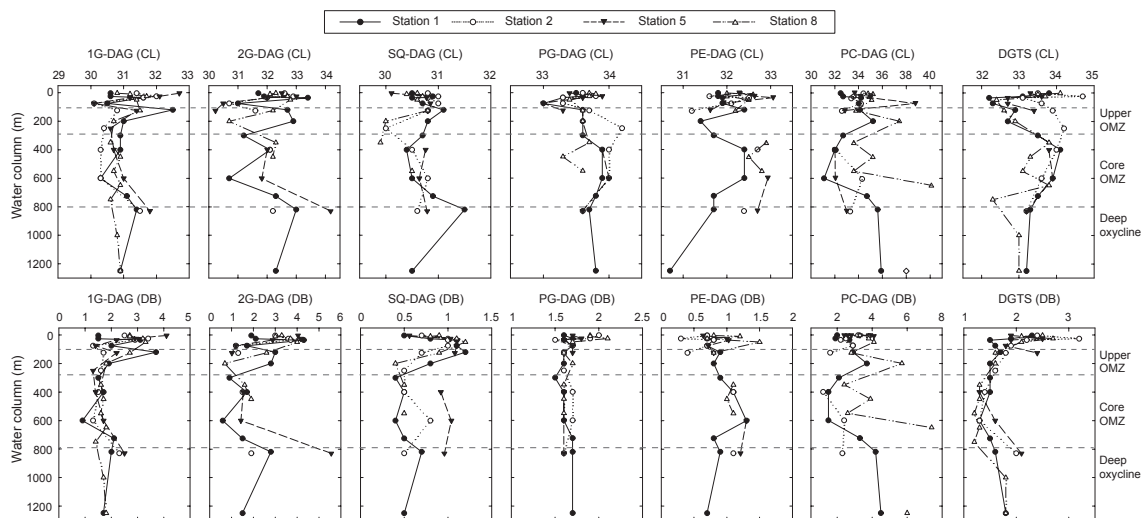




fig07

